NATIONAL AERONAUTICS AND SPACE ADMINISTRATION

Technical Report 32-255

An Experimental Correlation of the Nonreactive Properties of Injection Schemes and Combustion Effects in a Liquid-Propellant Rocket Engine

Part V. On the Influence of Vanes on Combustion and Combustion Stability

J. H. Rupe

JET PROPULSION LABORATORY
CALIFORNIA INSTITUTE OF TECHNOLOGY
PASADENA, CALIFORNIA

September 15, 1967

NATIONAL AERONAUTICS AND SPACE ADMINISTRATION

Technical Report 32-255

An Experimental Correlation of the Nonreactive Properties of Injection Schemes and Combustion Effects in a Liquid-Propellant Rocket Engine

Part V. On the Influence of Vanes on Combustion and Combustion Stability

J. H. Rupe

Approved by:

D. Dipprey, *Manager*
Liquid Propulsion Section

JET PROPULSION LABORATORY
CALIFORNIA INSTITUTE OF TECHNOLOGY
PASADENA, CALIFORNIA

September 15, 1967

TECHNICAL REPORT 32-255

Prepared Under Contract No. NAS 7-100
National Aeronautics and Space Administration

Contents

Figures

Contents (contd)

Figures (contd)

Abstract

Experimental observations of a high-amplitude resonant wave characteristic of several liquid-propellant rocket engine configurations are presented. These observations led to the postulate that the disturbance is a detonation-like wave that is not dependent upon the acoustic properties of the cavity for either initiation or sustenance and a consequential conclusion that the nonlinear properties of such processes must be elucidated as a first step in controlling this combustion mode. Results of a cursory evaluation of the control introduced by baffles (or vanes) and the heat-transfer rates imposed on the chamber walls for the resonant mode as compared to steady combustion are included.

An Experimental Correlation of the Nonreactive Properties of Injection Schemes and Combustion Effects in a Liquid-Propellant Rocket Engine

Part V. On the Influence of Vanes on Combustion and Combustion Stability

I. Introduction

During a series of experiments with liquid-propellant rocket engine injection schemes at the Jet Propulsion Laboratory (JPL), simultaneously maximizing uniformity of axial-mass-flux and mixture-ratio distributions invariably resulted in a resonant combustion mode characterized by a high-pressure ratio, high-frequency disturbance. Because the properties of these disturbances seemed to differ from those previously reported in the literature, a summary of these data was compiled, although the measurements were incidental to the main experiments and, hence, are severely limited in scope. It should be noted that the prime concern of the main investigation was to eliminate the disturbance so as to evaluate the injection schemes rather than the resonant phenomena.

These measurements were obtained as part of the Rocket Motor Injection Research Project, which was primarily concerned with the demonstration of the applicability of the nonreactive properties of injection schemes to the design of liquid-propellant rocket engines. The various aspects of this program were reported in Refs. 1 through 7 and are concerned respectively with the nonreactive properties of injection schemes and their application to injector design (Ref. 1), instrumentation and experimental techniques (Ref. 2), the performance evaluation (Ref. 3), chamber heat transfer (Ref. 4), starting transients (Ref. 5), the performance characteristics of high-flow rate elements (Ref. 6), and performance evaluation of the propellant system pentaborane and hydrazine (Ref. 7).

II. Experimental Apparatus and Techniques

Some nine different injection schemes and eight different propellant combinations were included in these studies. All experiments were conducted in a 40-L* uncooled engine with a contraction ratio of 2:1 from an 11-in. diam chamber that was intended to run at 300 psia to produce a nominal 20,000 lb thrust, when expanded to 13.5 psia (nominal ambient pressure at JPL's Edwards Test Station). Propellant flow rates varied with propellant combination, intended run mixture ratio, and experimental performance (C*). These rates were determined

from both venturi and turbine flowmeter measurements, but, generally, were not accurately known during the resonant combustion mode. The engine was instrumented with multiple transient-temperature plugs for heat-transfer measurements and multiple pressure transducers during all runs. High-response pressure measurements were obtained with Photocon equipment that is considered flat (± 5%) to approximately 10 kHz with low-response measurements (flat ± 1 dB) to 100 Hz being obtained with either Taber or Statham equipment. The most reliable information on the pressure characteristics of the resonant mode was recorded on a CEC Datatape using an FM system flat (± 5%) to approximately 10 kHz. Heat-transfer data (temperature-time histories) were recorded in some instances on an oscillograph; however, during the latter portion of the program, these data were recorded on a CEC micro-SADIC for automatic data reduction by the IBM 7090 computer. Reference 2 presents additional details of the instrumentation and control system, including a discussion of accuracies and capabilities. Additional details of the engine geometry are also given in Ref. 2, and geometrical and hydraulic properties of the injectors are given in Ref. 1.

Run durations for the nonresonant mode were from 2 to 3 s long and were monitored by a resonant-mode detector that initiated shutdown of the engine 50 to 150 ms after inception of the mode. Therefore, with a nominal 50-ms valve closure time, the total time of operation in the resonant mode was limited to approximately 200 ms.

III. Summary of Results and Conclusions

Measurements of the characteristics of the resonant-combustion mode were, for the most part, incidental and are, therefore, limited in extent. However, the pertinent observations or conclusions suggested by these experiments can be summarized as follows:

(1) The disturbance appeared to be a single front propagating in a predominantly circumferential direction that does not change once the front is established.

(2) The pressure-time and/or spatial characteristics of the disturbance at the combustion chamber boundary indicated a steep-fronted wave with pressure ratios across the front in the range of 5 to 10 and traveling at a velocity that nets an intersection velocity in the range of 6000 to 7000 fps, depending on propellant combination and injector configuration.

It should be noted that rise times were below the resolution capability of the pressure-measuring system so that the quantitative description of the amplitude of the disturbance is invalid (most probably too low).

(3) The heat transfer to the combustion chamber wall approached values of 16-20 Btu/in. s in the vicinity of the model plane station[1] (Ref. 1) during the resonant combustion mode. Comparative values of 0.5 to 1.0 Btu/in. s are obtained prior to the transition.

(4) Erosion rates tend to be localized in the same region for which the maximum heat transfer occurs and are estimated of the order of 2.5 in./s for an uncooled mild steel wall, after the wall temperature reaches approximately 2000°F.

(5) It was also cursorily indicated that the pressure ratio of the front varies with axial positions along the chamber, maintains a skewed intersection with the cylinder, and that the maximum amplitude is dependent upon the amount of propellant injected during the period of wave rotation.

(6) It was not possible in experiments with the fully developed resonant mode, where multiple simultaneous measurements were made, to reconcile the observations with the conventional description of the classical acoustical modes of the chamber, i.e., longitudinal, transverse, or rotating transverse mode.

(7) It was determined that a small number (3) of unequally spaced baffles would completely eliminate the resonant mode for all configurations evaluated.

IV. Discussion of Observations

A. Exploratory Records

Typical records of high-response measurements of the chamber-pressure fluctuations that were obtained during the early phase of the RMIR program are presented in Figs. 1 and 2. The steep-fronted characteristics of a high-amplitude disturbance was apparent even in these earliest measurements and the unfiltered analog of the disturbance includes a substantial contribution from some relatively high-frequency source. It was later shown that such

[1]The model plane is defined as the axial station at which the cross-sectional area of the spray for one of N elements is equal to $1/N \times (A_{CH})$.

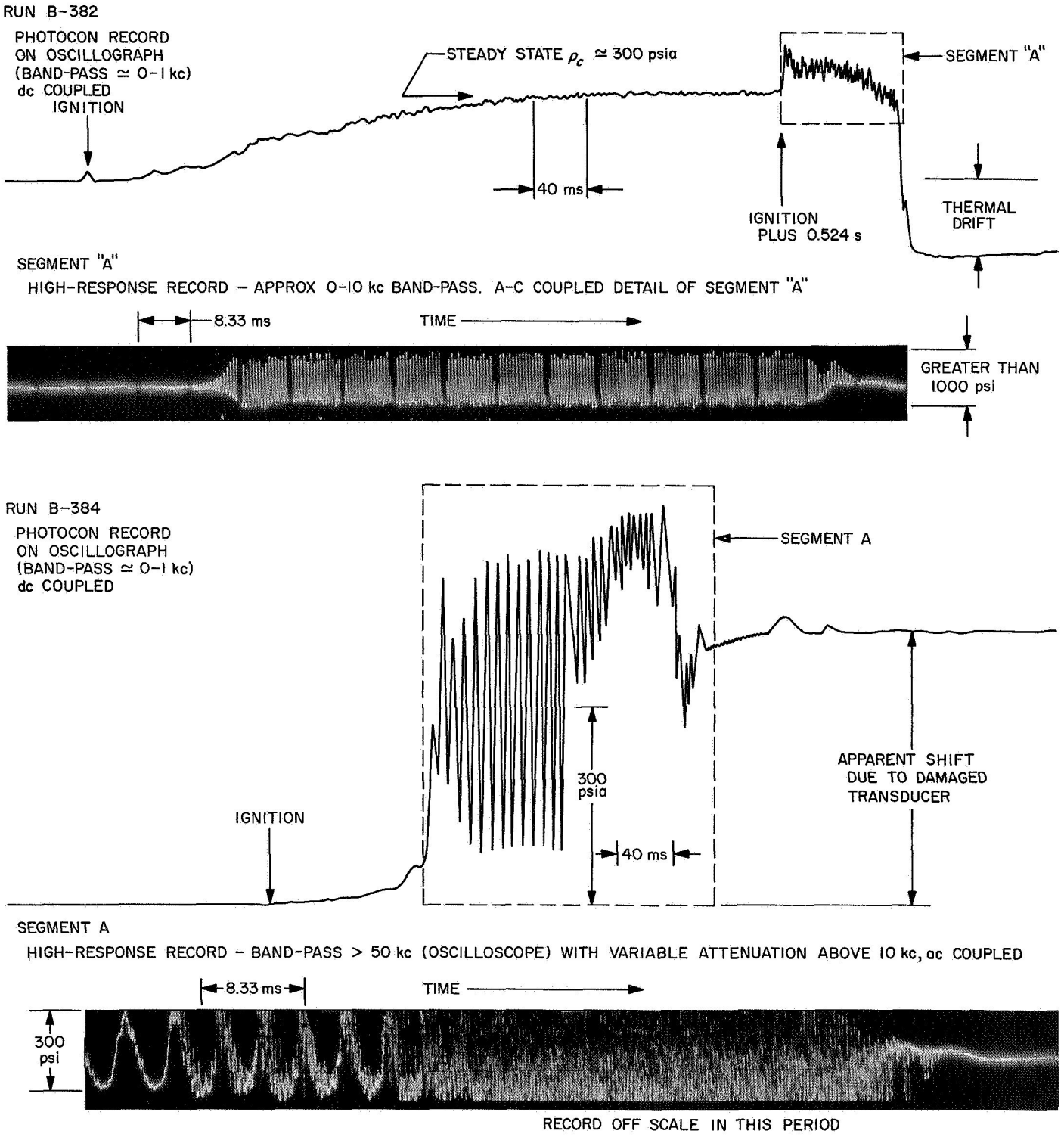

Fig. 1. Typical high-response records of resonant mode obtained in early RMIR injector experiments

records are quite misleading since the higher frequency components are probably caused by effects of acceleration upon the transducer (Refs. 7, 8, and 2).

Attempts to eliminate these disturbances by modifying the starting flow transient (because transition invariably took place during that time) were singularly unsuccessful, as indicated by the records identified as B-411 and B-412 in Fig. 2. In both cases, the manifolds were prefilled (by plugging the orifice exits with Teflon inserts that "popped out" as the manifold was pressurized) and the valve opening controlled to give, respectively, a very gradual flow transient and a very fast transient. It is seen that in both cases transition to the resonant mode was spontaneous even though the slow transient yielded a near steady-state chamber pressure before resonance was precipitated.

Because this combustion mode invariably resulted in intolerable heat-transfer rates and erosion rates at the boundary, particularly near the impingement point plane, some artificial damping was introduced to eliminate the disturbance. As indicated in Fig. 3, the erosion was concentrated along the first 2 to 3 in. of the chamber wall (immediately downstream of the injector face) and, in the case of the *Corporal*-like injectors (Ref. 1), along the outer portions of the injector face and including the external surfaces of the orifice extensions. It was noted that the downstream portion of the orifices was relatively unaffected, as was the center portion of the injector face. Therefore, it was concluded that the most severe environment, insofar as the boundaries are concerned, is concentrated in an annular volume bounded by an inner radius of some 3 in., the chamber wall, and a downstream surface located 2 to 3 in. from the injector face. This observation is consistent with the concept of a longitudinal acoustic mode of disturbance if the nonerosive condition near the axis of the injector face is rationalized by noting that little or no propellant is injected into that region. However, it is difficult to see how such a disturbance could produce a tangential force on the orifice extensions as evidenced by the preferential direction in which bending failure occurred (Fig. 3). Therefore, it was concluded that the dominant forces associated with the disturbance had a substantial tangential component and could be effectively damped with radial baffles or vanes[2]. These baffles should not affect the longitudinal characteristics of such disturbances.

[2]The use of vanes/baffles for this purpose has not been highly publicized but appears to have been used at least as early as 1954 by Male and Kerslake of the NACA (Ref. 21).

B. Baffle Configuration

The first installation of baffles on the RMIR Injector 1 (Ref. 1) was accomplished as shown in Fig. 4a by removing three sets of orifices and welding three relatively thick baffles to the injector face. A nonrepetitive spacing was chosen to minimize the probability of any harmonic coupling between the several cavities that were formed. The baffles extended to a common axial station that was 0.5 in. beyond the model plane. Although it was obvious that the baffle would interfere with the adjacent sprays, it was not possible to associate any quantitative significance to this effect. In subsequent analyses, it was assumed that the associated modification of mass and mixture ratio distributions had a negligible effect on the experimental observations.

In the first experiments with this baffled injector geometry, smooth combustion was achieved for a 2-s run, using *Corporal* propellants with a dual-action blade valve that was intended to control the starting transient. Consequently, it was concluded that the disturbance had been traveling in the tangential direction and could be adequately damped with this three-baffle geometry. However, in the attempt to duplicate the experiment, a spontaneous transition to the resonant mode occurred after 1.16 s of steady operation to produce the record identified as B-419 in Fig. 2. It should be noted that (1) the transition appears to take place over a relatively long time as indicated by the gradual buildup of the disturbance, (2) that the peak amplitude is substantially reduced compared with amplitudes obtained without baffles, but that (3) the frequency relative to the unbaffled experiments was essentially unchanged. Further, in a completely qualitative observation, it was also noted that the surfaces upstream of the baffles were coated with a deposit that is typical for the *Corporal* propellant system burning in a cold-wall chamber while the downstream portion of the chamber wall was exceptionally clean. This latter observation infers that the disturbance has a predominately circumferential motion and, in this case, appears bounded by the downstream edge of the baffle. Because of the marked change in the amplitude of the disturbance with the initial baffle installation, it seemed reasonable to expect additional attenuation with additional baffle length. A 1-in. extension was welded to the original baffle, as shown in Fig. 4b, to produce a completely stable combustion system for the nine subsequent tests, i.e., chamber pressure fluctuations of less than 1% of the mean pressure over a range of mixture ratios and various ignition conditions. These tests completed the performance evaluation of that particular injector. They were followed by an additional 40 tests with injectors of similar

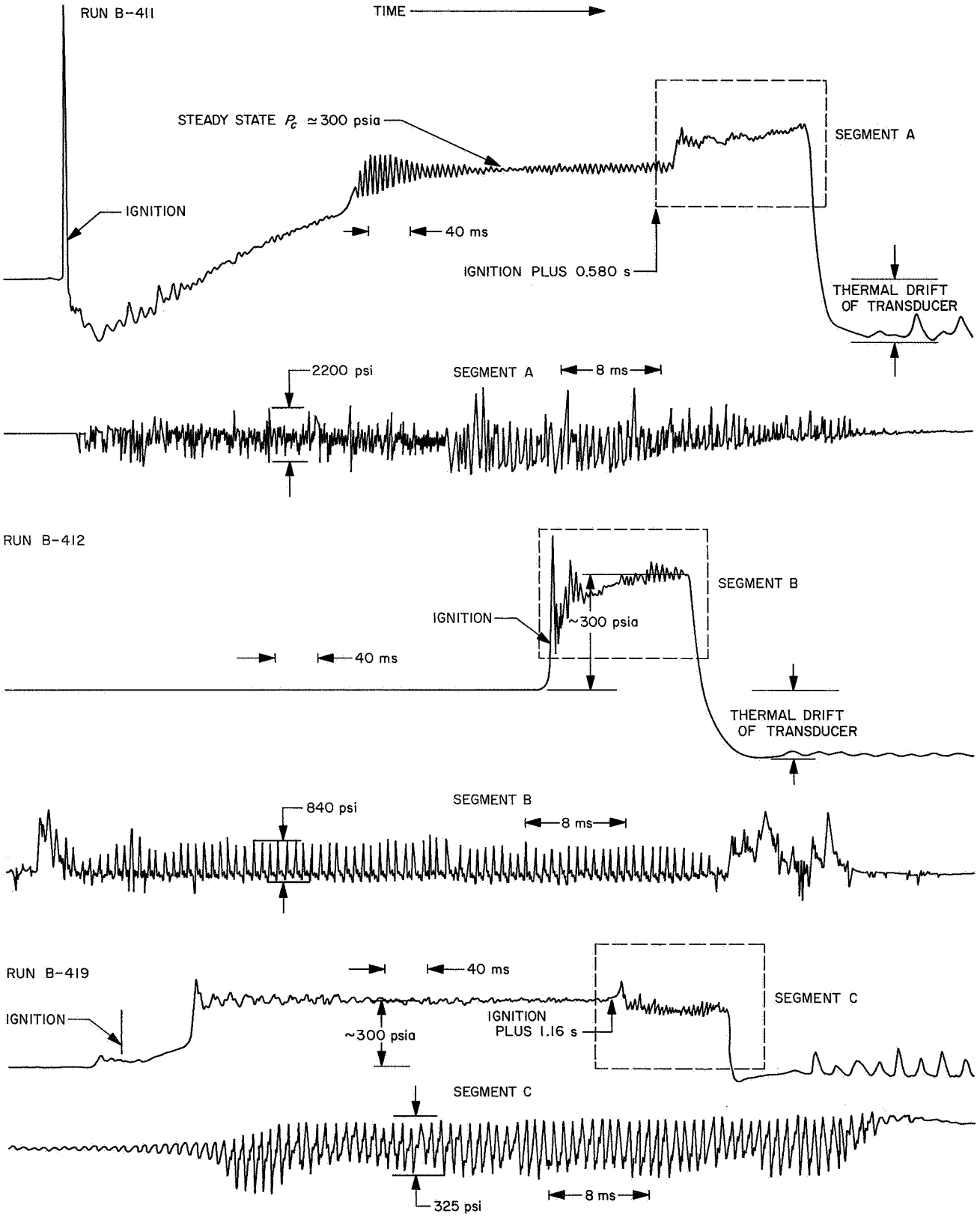

Fig. 2. Transition to resonant mode—RMIR Injector 1 with *Corporal* propellants

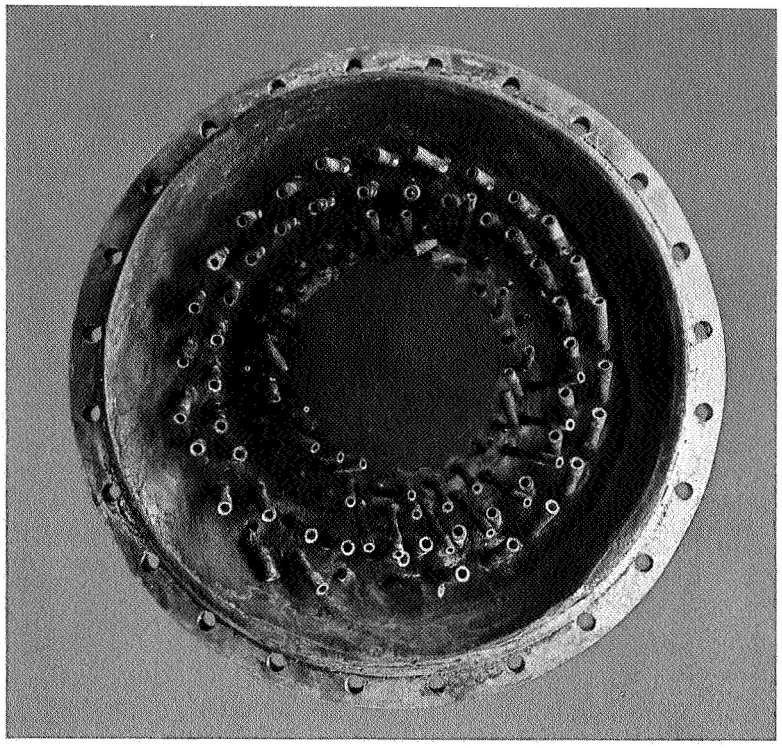

(a) INJECTOR FACE EROSION

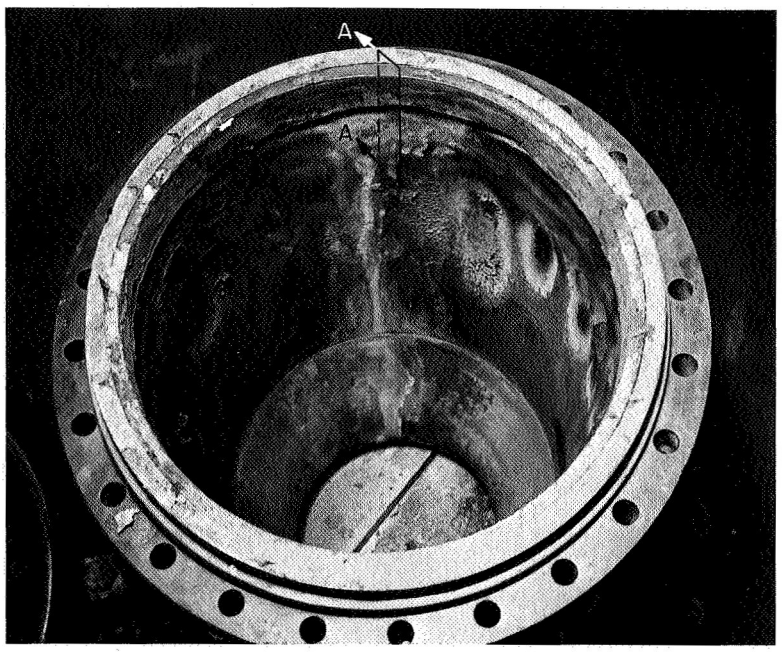

(b) INJECTOR-END EROSION PATTERN

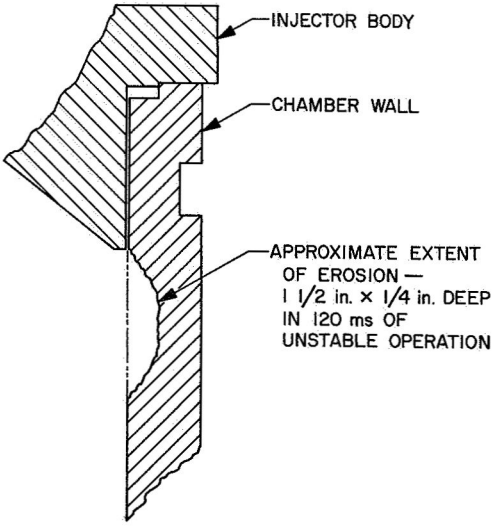

SECTION A-A

Fig. 3. Erosion due to resonant combustion—*Corporal*-like injector and uncooled mild steel chamber

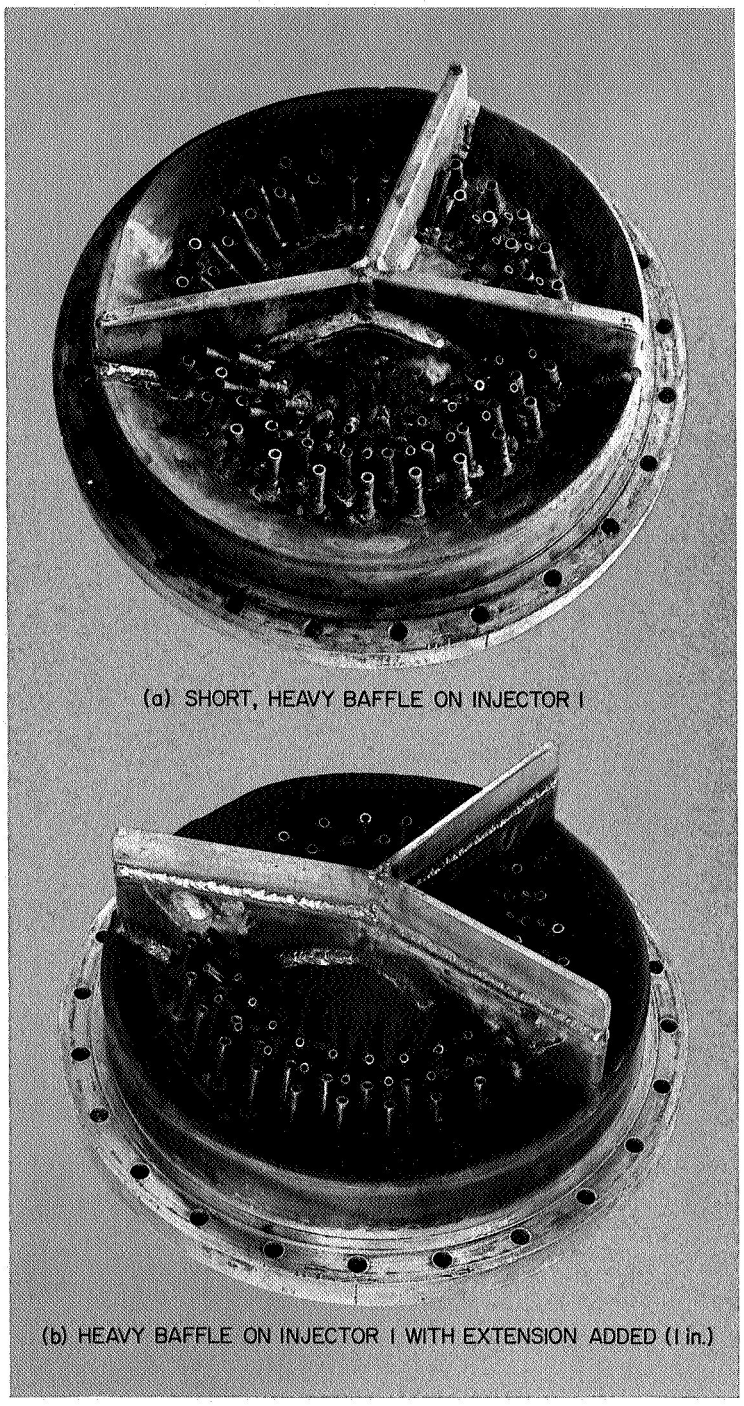

Fig. 4. Baffle installation on RMIR Injector 1

geometries (RMIR Injector 2, 3, and 4 with baffles) that exhibited the nonresonant combustion mode with the exceptions described in the following paragraphs.

C. Baffle Erosion

In three separate instances the transition to the resonant mode was initiated spontaneously because of baffle erosion along the joint between the baffle and the injector face. All of the installations subsequent to Injector 1 were susceptible to this process because of the discontinuous weld at the injector face. These limited experiences indicated that the erosion was progressive with accumulated run time, and that the transition would be spontaneous once the hole in the baffle was of the order of 1 to 2 in.^{2} The size of an opening that is adequate for initiation of such a disturbance is shown in Fig. 5 although it should be noted that part of the baffle damage was undoubtedly sustained during the resonant combustion mode. The amplitude of the observed disturbances in these instances increased in a gradual manner to peak-to-peak values in the range of 600 psi with a dominant frequency at approximately 1800 Hz.

D. One Baffle Deleted

In an effort to ascertain the significance of the three-baffle geometry, one injector was constructed so that any one, two, or all baffles could be deleted. However, only one alternate configuration was evaluated with the No. 3 baffle deleted as shown in Fig. 6, after it was found that the resulting two-baffle arrangement would allow a spontaneous transition to the resonant mode. In this case, the dominant frequency appeared to shift to approximately 3500 Hz while the amplitude was limited to a value in the range of 150 psi peak-to-peak. The fact that the frequency appeared nearly double that of the unbaffled geometry may have been caused by the additional complexity of the disturbance, or reflections from the baffle surface, rather than the sudden appearance of some new, ill-defined acoustic mode.

In addition to these observations with *Corporal*-like injectors, a limited number of interim measurements were obtained with RMIR Injectors 5 and 7. Ultimately, several more definitive experiments were conducted with those particular injectors. The interim measurements checked stability without baffles prior to the performance evaluation. The latter tests were intended to yield, insofar as possible, simultaneous quantitative amplitude and phase measurements for several circumferential positions at each of two axial stations. Finally, some limited observations were obtained with (1) a relatively large element injection scheme (RMIR Injector 8), and (2) one of the above injectors (RMIR Injector 7) replumbed to give like-on-like injector elements.

E. Baffle Length vs Resonance

1. RMIR Injector 5. Injector 5 was designed to produce near-uniform axial mass flux and mixture ratio distributions with *Corporal* propellants at a mixture ratio of 2.80. The initial performance evaluation of this injector was conducted without baffles and, as shown in Fig. 7,

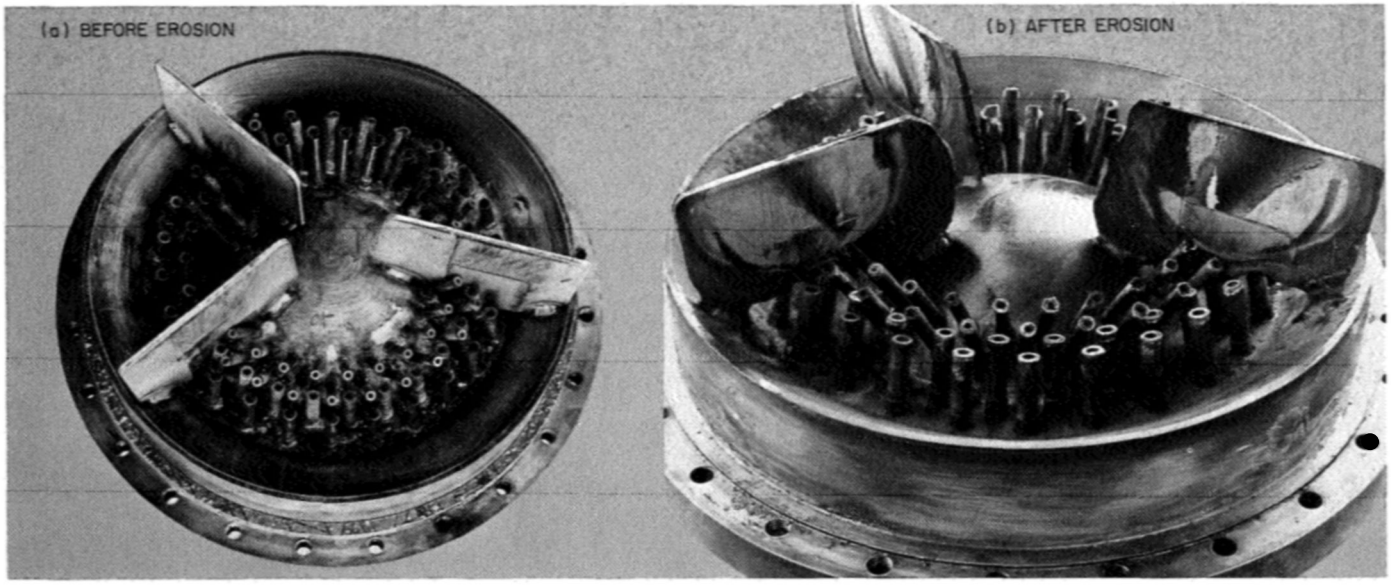

Fig. 5. Baffle erosion that allows resonant mode—RMIR Injector 3 (Run B-445)

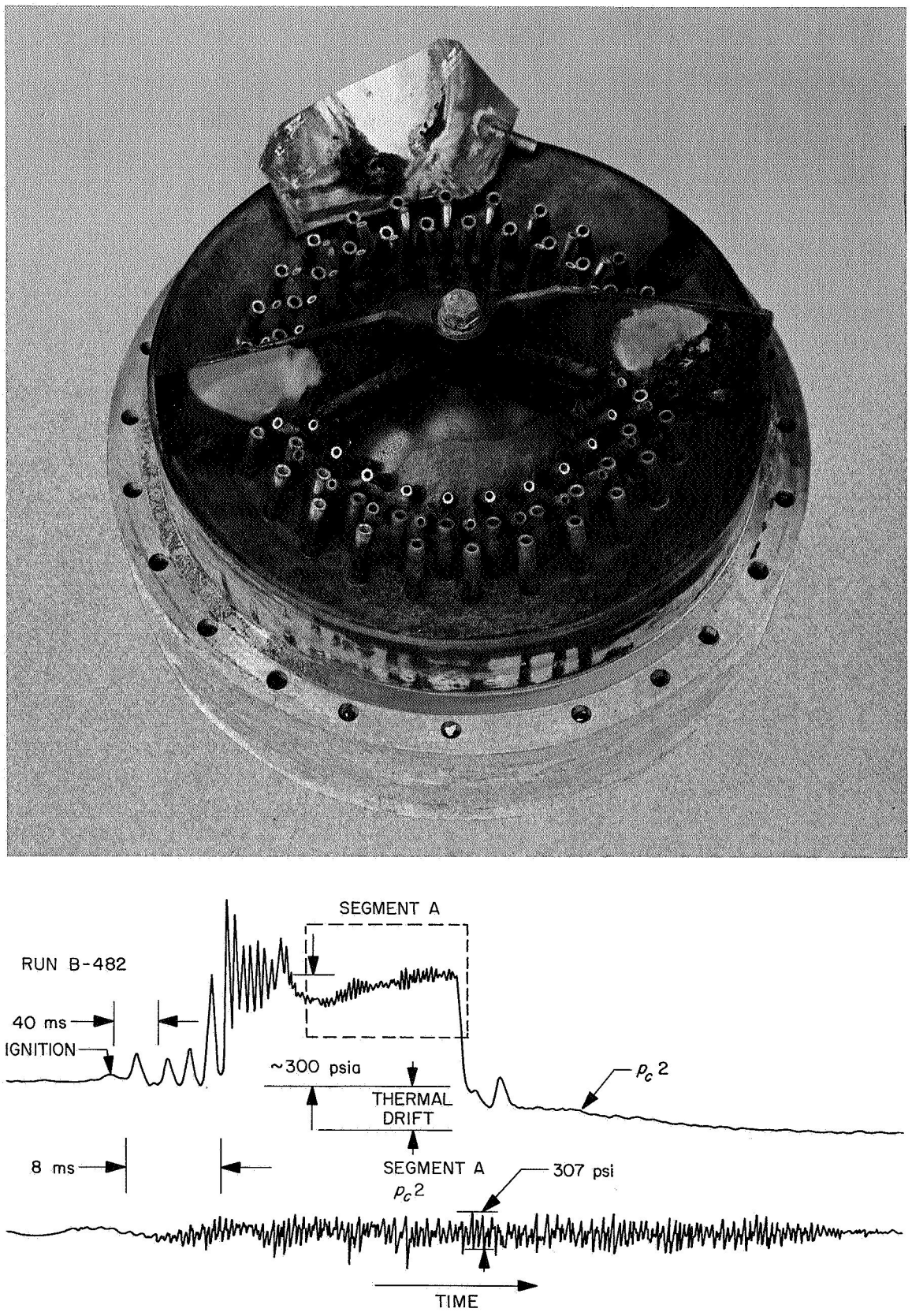

Fig. 6. RMIR Injector 3 with No. 3 baffle deleted (Run B-482)

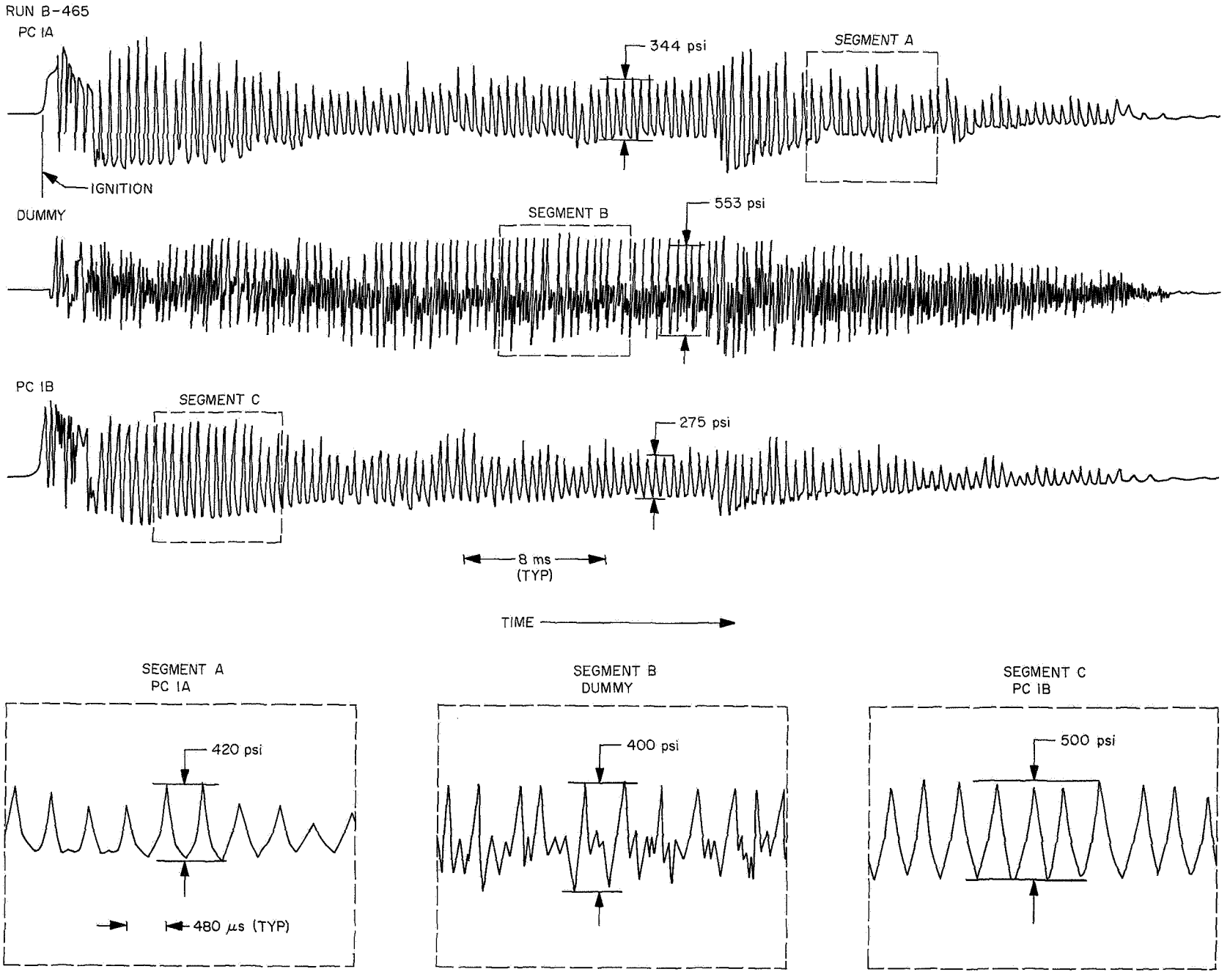

Fig. 7. Spontaneous transition to resonant mode during starting transient—RMIR Injector 5 with *Corporal* propellants (B-465)

underwent spontaneous transition to the resonant mode during the start transient. It is interesting to note that not only was the disturbance at its full amplitude when it was first detectable (at the wall) but that a "dummy" transducer, which was similarly mounted but not exposed to chamber pressure, yielded an analogous output from the effects of acceleration alone. The run was nominally 120 ms long and indicated a resonant frequency of approximately 2 kHz with peak amplitude in the order of 2000 psi (as measured on the injector face plane). It should be noted that it was ultimately shown (after the performance evaluation was completed) that this transition was initiated by the start transient and, at least for mixture ratio values near 2.80, this injection scheme has a substantial stability margin. However, with the starting sequence used at that time (Ref. 5), it was necessary to install baffles as shown in Fig. 8a. In this case, they extended approximately to the model plane (2¼ in. from the face) and were intended to be geometrically similar to the previous injectors, i.e., in the sense that there are three unequally spaced, near-radial baffles. The actual placement on the injector face was further dictated by an attempt to minimize interference with the injector elements.

The performance evaluation of that geometry yielded a spontaneous transition to the resonant mode at ignition as before, but the frequency appeared to be reduced somewhat, to approximately 1875 Hz, and the amplitude substantially reduced to approximately 156 psi peak-to-peak. An oscillograph trace of this run (B-493) is included in Fig. 8c for comparison with the unbaffled disturbance. Again, as with the *Corporal*-like injectors, 1 in. was added to the length of the vane (Fig. 8b). This addition again produced a completely stable system. The significance of these experiments is illustrated in Fig. 9, which shows the variations of the amplitude of the disturbance (at a particular point on the combustion chamber boundary) with baffle length. Clearly, the influence of the baffle (the amount of attenuation) is proportional to baffle length in a nearly exponential manner over some finite chamber length that must contain the so-called sensitive region. It is intuitively obvious that this sensitive length (volume) is dominated by the injection scheme in the sense that it is the injection parameters that control mixing rates, composition, and rates of heat transfer to the propellants. Hence, generalization of the data shown in Fig. 9 to other injectors would require a normalization based on the relative location of those dominant parameters. Further, the baffles protect the early combustion processes within a cavity that cannot be resonantly coupled with the characteristic combustion process and, therefore, the effectiveness of such a device depends upon achieving a substantial part of the combustion process within a cavity having a relatively complicated geometrical configuration.

2. RMIR Injector 7. RMIR Injector 7 is similar to Injector 5, except that it incorporates 47 elements of a geometry different from that of the 52 elements making up Injector 5. These modifications were required to satisfy the uniformity criteria (mass and mixture ratio distributions) for the propellant system $N_2O_4 + N_2H_4$ (Ref. 1).

The initial performance evaluation of this injector-propellant combination without vanes was singularly unsuccessful because: the engine was unstable from the start (inferred from erosion and heat-transfer data), the resonant cutoff device failed to terminate the run (because of a control wiring error), no high-response pressure records were obtained (because of a patch error), and the injector suffered moderate damage in the subsequent extended run. Therefore, no data on amplitudes and frequency of the disturbance were available until completion of the performance evaluation. For this interim period, 3.55-in.-long baffles (1 in. beyond the model plane) were installed as shown in Fig. 10 in an attempt to achieve stable operations. Although there was really no evidence of resonant combustion for this baffle configuration, this particular propellant combination consistently produced relatively rough combustion. Quantitatively, this meant that the RMS value of the fluctuation was approximately 11 psi at the design mixture ratio with peak-to-peak variations of approximately 70 to 80 psi (with a mean chamber pressure of approximately 300 psi).

The influence of vane length upon the spontaneous transition to the resonant mode was evaluated by varying the vane length for a constant gross mixture ratio with the standard element configuration (unlike impinging streams). In one test with Injector 7, a fourth vane was added (to divide the larger cavity) and the overall length of all vanes was actually increased to 4.70 in. to determine if the noiselike characteristics of the combustion process could be attenuated. This experiment was negative; no change in the combustion characteristics was detectable. Subsequently, the vane length was shortened to 1.85 in. and the combustion characteristics were reevaluated prior to removing the vanes completely.

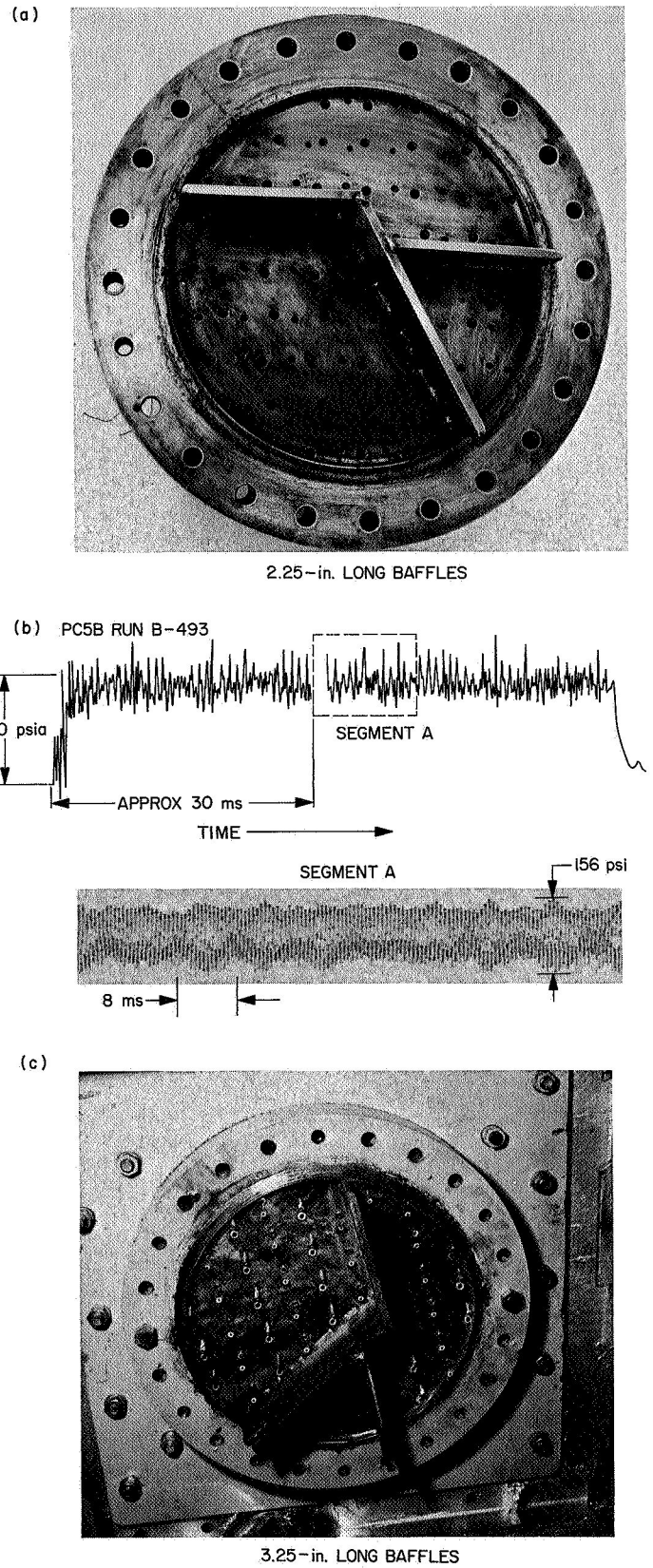

Fig. 8. Baffle installation on RMIR Injector 5

In the case of that intermediate length vane, a truly dominant frequency at about 2250 Hz became apparent as indicated in the spectrum analysis for that configuration which is presented in Fig. 11. Further, it was noted that the RMS value for this disturbance increased (in comparison with the fully baffled configuration) to approximately 21 psi with peak amplitudes in the range of 150 ±15 psi. Finally, when the vanes were removed completely, the frequency of the disturbance increased to approximately 2400 Hz (Fig. 11), the RMS value of the fluctuation increased to approximately 150 psi, and the peak amplitude was in the range of 600 ±100 psi. As with Injector 5 and *Corporal* propellants, the intermediate length baffles allow intermediate

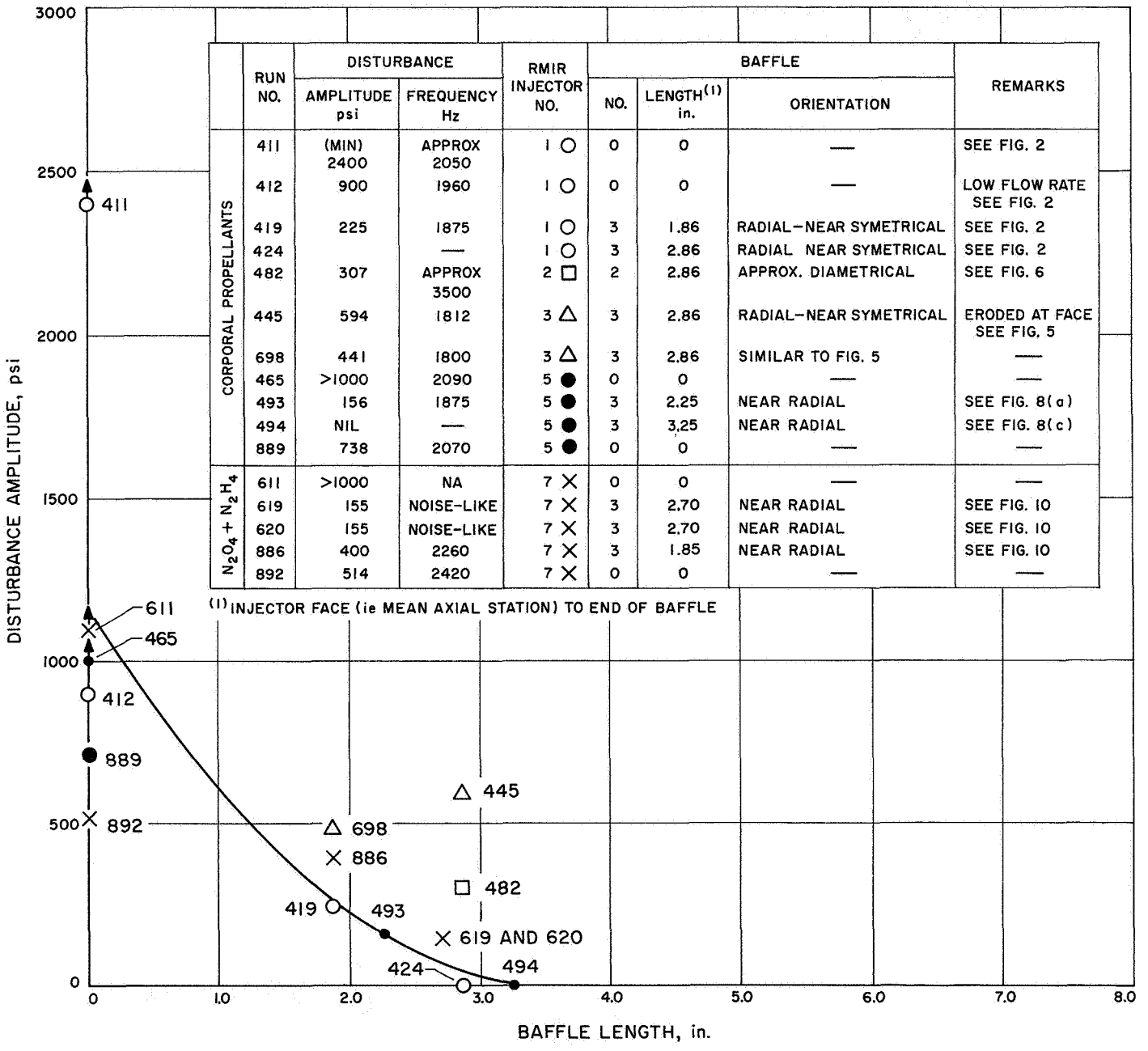

	RUN NO.	DISTURBANCE AMPLITUDE psi	DISTURBANCE FREQUENCY Hz	RMIR INJECTOR NO.	BAFFLE NO.	BAFFLE LENGTH(1) in.	BAFFLE ORIENTATION	REMARKS
CORPORAL PROPELLANTS	411	(MIN) 2400	APPROX 2050	1 ○	0	0	—	SEE FIG. 2
	412	900	1960	1 ○	0	0	—	LOW FLOW RATE SEE FIG. 2
	419	225	1875	1 ○	3	1.86	RADIAL–NEAR SYMETRICAL	SEE FIG. 2
	424		—	1 ○	3	2.86	RADIAL NEAR SYMETRICAL	SEE FIG. 2
	482	307	APPROX 3500	2 □	2	2.86	APPROX. DIAMETRICAL	SEE FIG. 6
	445	594	1812	3 △	3	2.86	RADIAL–NEAR SYMETRICAL	ERODED AT FACE SEE FIG. 5
	698	441	1800	3 △	3	2.86	SIMILAR TO FIG. 5	—
	465	>1000	2090	5 ●	0	0	—	—
	493	156	1875	5 ●	3	2.25	NEAR RADIAL	SEE FIG. 8(a)
	494	NIL	—	5 ●	3	3.25	NEAR RADIAL	SEE FIG. 8(c)
	889	738	2070	5 ●	0	0	—	—
$N_2O_4 + N_2H_4$	611	>1000	NA	7 ×	0	0	—	—
	619	155	NOISE-LIKE	7 ×	3	2.70	NEAR RADIAL	SEE FIG. 10
	620	155	NOISE-LIKE	7 ×	3	2.70	NEAR RADIAL	SEE FIG. 10
	886	400	2260	7 ×	3	1.85	NEAR RADIAL	SEE FIG. 10
	892	514	2420	7 ×	0	0	—	—

(1) INJECTOR FACE (ie MEAN AXIAL STATION) TO END OF BAFFLE

Fig. 9. Baffle length vs disturbance amplitude (Injectors 5, 1, and 7)

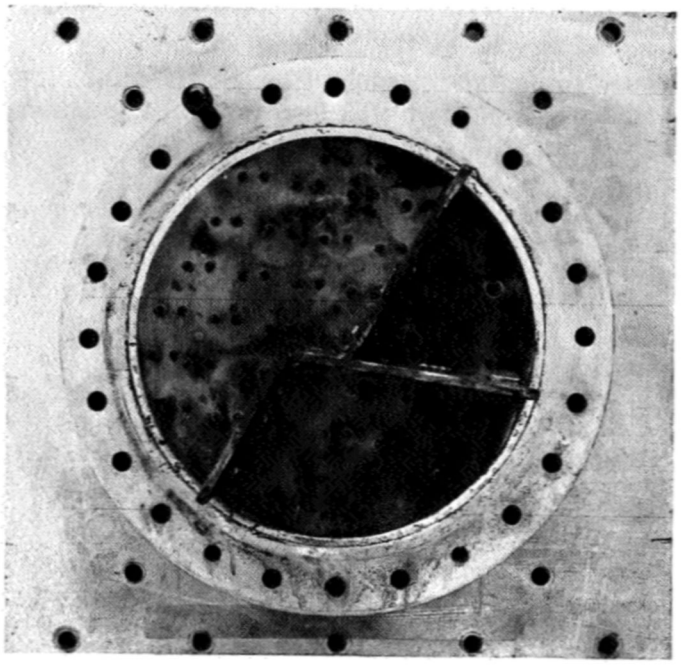

Fig. 10. Baffle Installation on RMIR Injector 7 (B-578 through B-581)

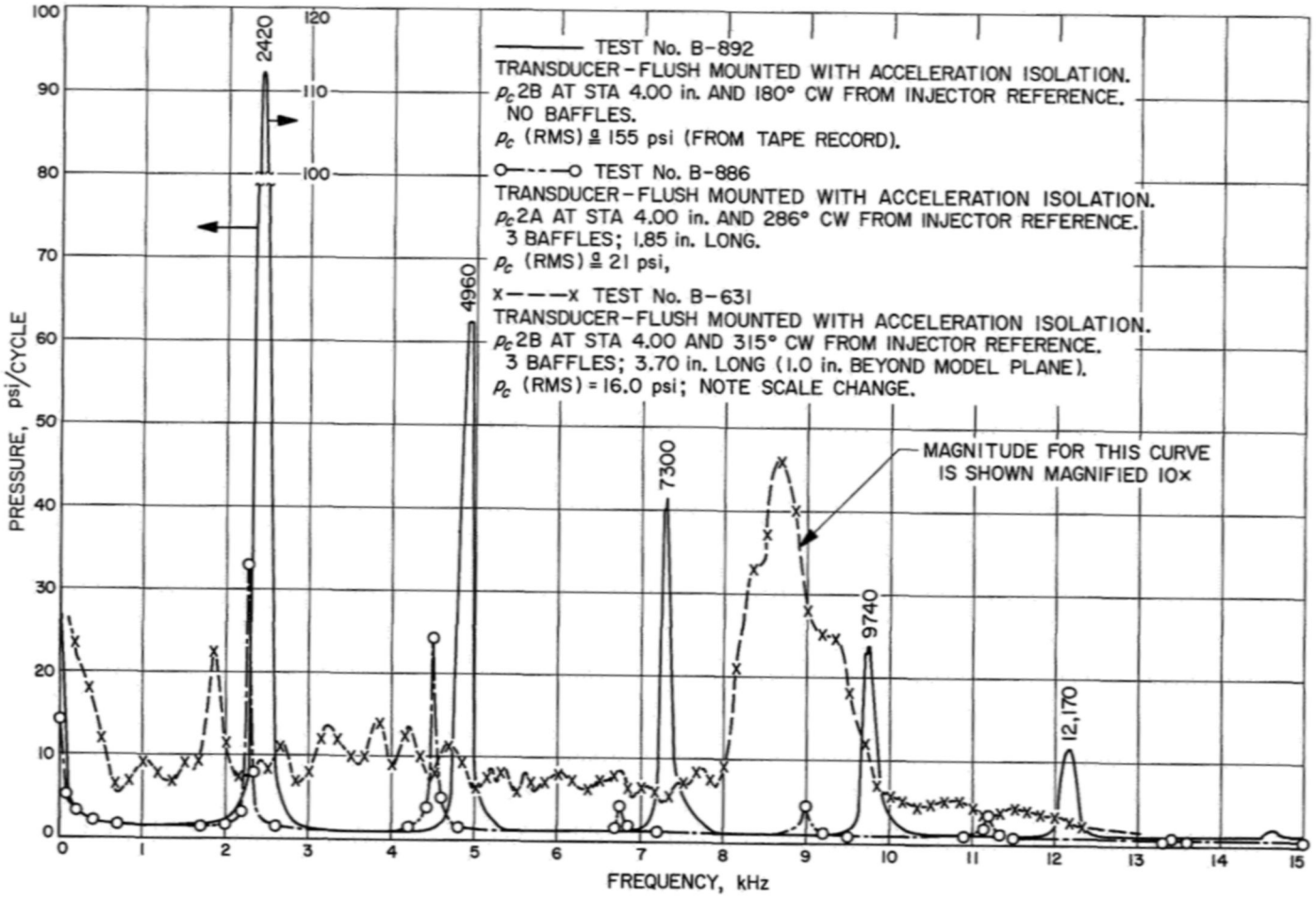

Fig. 11. Spectrum analysis for RMIR Injector 7 with $N_2O_4 + N_2H_4$ with and without baffles

intensities in comparison with the fully developed disturbance that was attained without baffles.

F. Rough Combustion of N_2H_4 Fuel Systems

1. General. The pressure fluctuations observed for this system with vanes installed were noiselike in character because they exhibited a near-uniform distribution of energy over the frequency range that could be recorded. A spectrum analysis of a typical pressure record for this system is shown in Fig. 11 (B-631). The figure shows that the energy swell near a frequency of 8700 Hz is nearly three times the average but even so represents a small fraction of the total energy and should not be construed as a dominant or characteristic frequency. This becomes particularly clear if this distribution is compared with a similar analysis of B-892 which was obtained from the truly resonant mode (without vanes) and is superimposed on the analysis as described above. It should be noted that the $10\times$ amplitude-scale-factor is used to display the nonresonant disturbances.

It should be noted that this noiselike characteristic of the pressure measurement (B-631) was encountered in nearly every test using N_2H_4 as the fuel and either acid or N_2O_4 as the oxidizer, and that the integrated intensity (RMS average) was mixture ratio dependent as reported in Ref. 9. These data, reproduced in Fig. 12, illustrate that, with either N_2O_4 or SFNA oxidized propellant systems and two different injectors (RMIR Injectors 5 and 7), the intensity of the disturbance increases as mixture ratio decreases, i.e., as the mass fraction of hydrazine increases. Therefore, it is suggested that the high-roughness level is, in some way, associated with the relatively high concentration of hydrazine and that, perhaps, the locally high concentrations of hydrazine are particularly pressure sensitive and can produce local detonations partly caused by thermal decomposition of that component.

Another significant point concerning rough combustion is illustrated by comparing the data of Figs. 12a and 12b. The correlation between relatively high performance and high intensity for the disturbance is unmistakable. Roughness can contribute to combustion efficiencies and, hence, must be considered in any absolute comparison of quantitative values.

2. Exceptions to rule. Although the N_2H_4-fueled propellant systems seem to be characterized by relatively rough combustion, it should be noted that there are at least two exceptions. First, in some small-scale experiments at a nominal 100-lb thrust level, Rowley (Ref. 10) reported extremely smooth combustion with these propellants and unlike impinging injectors (± 4 psi peak-to-peak at a chamber pressure of 150 psi). Also, as part of the RMIR program (Ref. 3), Injector 7, as described above, was modified (by replumbing the upstream manifolding) to produce a 47-pair like-on-like impinging stream injector that produced markedly different combustion characteristics. With this latter configuration, the RMS pressure fluctuations were decreased to negligible values (baffles were retained) during most of the 2 to 3 s of a typical run.

However, during several of the higher mixture ratio runs with this latter configuration (3 out of 5 runs at mixture ratios from 0.970 through 1.437), it was noted that, at random times during particular tests, an extremely high-amplitude burst of highly damped, though presumably resonant, pressure fluctuations would occur. The initial front would appear instantaneously and would have an amplitude in the order of 350 to 700 psi above mean chamber pressure. This amplitude would then decay in an oscillatory fashion to a negligible value over a period of approximately 100 ms. This event did not appear in some of the tests, while in others, it occurred from one to three times during a 2.5- to 3-s run and could not be related to any other event. Because of this fact, and because the performance produced by this injection scheme was degraded some 3.5 to 4%, the investigation of this phenomenon and its association with this injection scheme was not pursued. It should be noted that this decrease in relative performance is consistent with the premise that roughness must be considered in any comparison of relative performance of different engines and/or operating conditions and had the same quantitative decrement that might have been predicted from Fig. 12.

G. Resonance Characteristics of RMIR Injector 8

During the performance evaluation of the high thrust per element injector of RMIR Injector 8 (see Ref. 1 for the nonreactive properties and design specifications for this injector and Ref. 6 for additional information on the performance characteristics of the engine) a more or less continuous transition from a nominally noiselike character to the fully resonant mode was observed as run time was accumulated on the injector. In the first five runs with the injector, during which mixture ratio (hence oxidizer flow rate) was varied from 1.20 to approximately

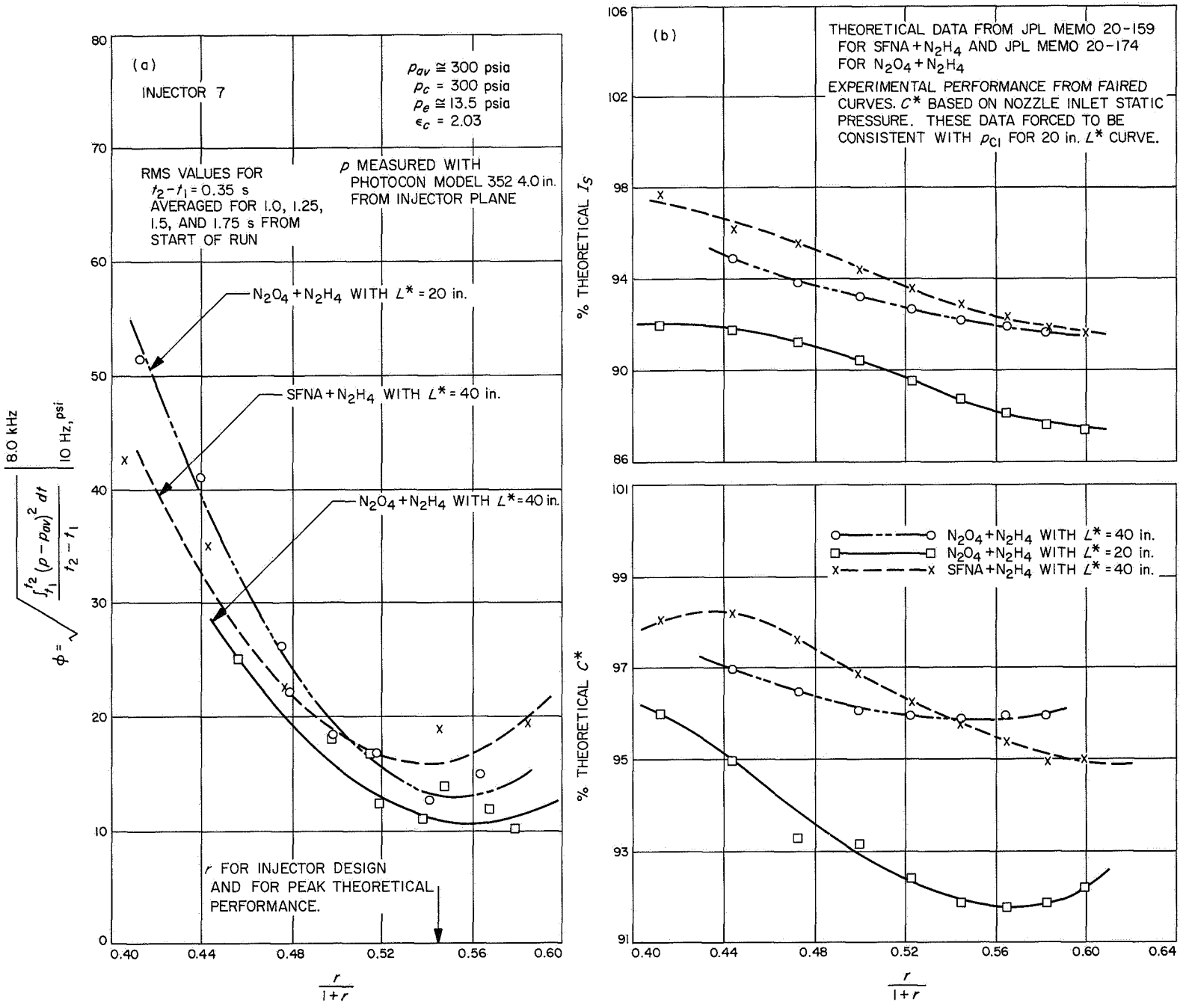

Fig. 12. Combustion noise vs performance with N_2H_4 as fuel

1.50, nonresonant combustion was achieved without baffles although the RMS pressure fluctuations were in the order of 7 to 14 psi. Because of the experience with the 47-element injector with the same propellants, fluctuations of this magnitude were expected and it was rather surprising that they did not initiate the transition to the resonant mode. However, as the mixture ratio decreased (mass fraction of hydrazine increased), and sporadic bursts of a high initial amplitude but highly damped resonance were observed. These disturbances were similar to those obtained with the like-on-like configuration of Injector 7 with one notable exception. With RMIR Injector 8, the frequency of appearance of these bursts increased with total run time until, after some 20 s of accumulated run time, a near steady state resonant mode was established. Under these conditions, the RMS value for the fluctuations was in the order of 60 psi (peak-to-peak $\triangleq$ 240 psi) with a dominant frequency of 2015 Hz. Similar characteristics were also observed in a final experiment with this injector configuration even though the mixture ratio was changed to a value for which steady combustion had been achieved previously.

As noted in Ref. 1, this injector incorporated a number of vaned elbows as integral parts of the oxidizer orifices. To resolve the possibility that the disturbances might be aggravated by a gradual failure of these vanes producing cavitation or gross disturbances in the jets (which was later shown to be the case), the orifices were replaced by simple straight tubes 50 diameters long, fed by flexlines with an inside diameter of 0.406 in. that were approximately 100 diameters long. This configuration gave approximately 1.3 s of nonresonant combustion before a transition to resonance so that the installation of baffles seemed essential. This installation was accomplished as shown in Fig. 13 and yielded a system that was nonresonant (although rough) for the subsequent 52 short-duration (2 to 3 s) tests which covered a range of mixture ratios for the N_2O_4 + UDMH propellant combination as well as N_2O_4 + N_2H_4 and for two different chamber lengths (16 and 32 in.) to give L^*'s of approximately 40 and 72 in.

It was also noted that the intensity of the pressure fluctuations (RMS value) for this injection scheme using UDMH as the fuel (six elements for nominal 20,000-lb thrust) was essentially the same as for hydrazine as well as being similar to the values observed for RMIR Injector 7 with $N_2O_4 + N_2H_4$ (Ref. 9). This observation is significant because it was the only injection scheme in which UDMH failed to produce a low level of combustion noise regardless of injector geometry, mixture ratio, or oxidizer. There

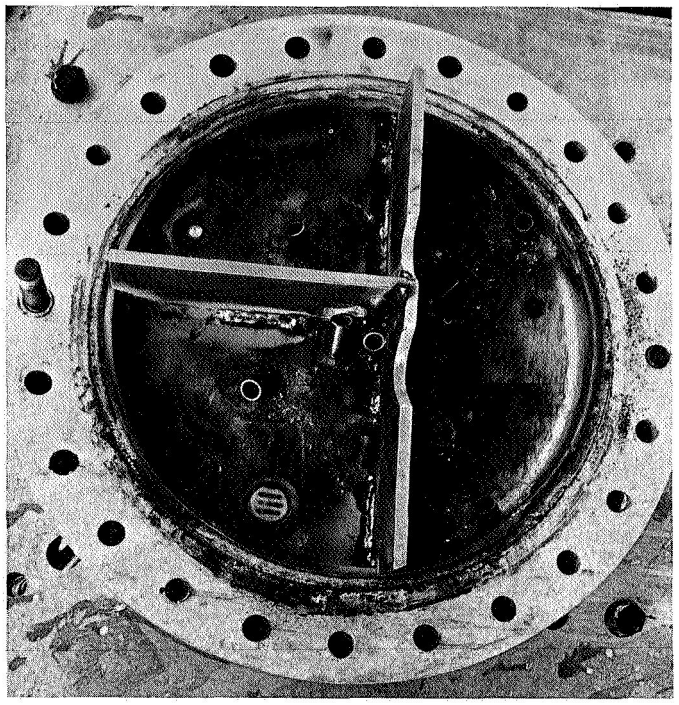

Fig. 13. RMIR Injector 8 with baffles

is no real explanation for this observation. However, it is reasonable to expect that the phenomenon is directly related to the substantial differences in mass and mixture ratio distributions that are produced by these two injectors. This again points to the possibility that the monopropellant characteristics of these fuels may lead to exceptionally sensitive centers of decomposing propellant.

H. Oscillatory Behavior of the *Corporal* Injector

A distinctly different mode of resonant combustion was encountered in the case of the *Corporal* injector with *Corporal* propellants where a relatively low frequency, in the range of the 140 Hz, though moderate amplitude (75 to 230 psi) fluctuation was observed throughout the intermediate mixture ratio range. With the limited data available, it appears that the maximum amplitude occurs at a particular mixture ratio of approximately 2.50 and damps out completely at mixture ratios below approximately 2.23. It is most likely that the absolute value of mixture ratio is of little or no consequence but simply reflects a set of critical parameters that includes jet velocities, resultant momentum angles, injector pressure drop, and so forth, which in turn control system characteristics as well as mass and mixture ratio distributions.

Because this resonant frequency is only ¼ of the fundamental frequency for the axial mode of this cavity (based

on classical acoustics and a realistic sound velocity), it seems that the resonance must be caused by coupling between combustion characteristics for the injector, chamber, propellant combinations, and system dynamics (chugging in the context of the Crocco and Cheng analysis in Ref. 11). This conclusion is also brought out by the appearance of the shock diamond in the exhaust of this engine which, during this resonant mode, was alternately characteristic of an overexpanded and then underexpanded nozzle flow and, hence, consistent with the concept of a nearly uniform pressure throughout the chamber. Although this combustion mode was not observed with the *Corporal*-like injectors with long orifices, it should be noted that the pressure drop across those injectors increased some 2 to 2.5 times and, hence, would be expected to contribute to systemic stability.

I. Resonance Characteristics with Unbaffled Injectors

In an attempt to determine the mode of the disturbance encountered with Injectors 5 and 7, a few experiments were conducted with the same engine configuration used for the performance measurements, except that all baffles were removed from the injectors. These were the last experiments conducted to determine the influence of baffle length on characteristics of the disturbance. The most important difference for these tests was in the number of high-response transducers for which simultaneous measurements were obtained. As indicated in Figs. 14 and 15, the transducer orientation was somewhat different for the two injectors; however, in both cases, not less than two measurements were obtained on the injector face and two other measurements at a given station on the chamber. In one instance, a dummy transducer was also installed on the chamber at that same axial station.

All chamber transducers were flush-mounted, type 352 Photocons installed in soft mounts for vibration isolation; injector transducers were hard-mounted, type 307 Photocons. It is believed that, in the latter case, acceleration effects are negligible because of the rigidity of the thick, stiff injector plates (2.5-in. thick mild steel). Transducers were flush to the inner face of Injector 7; however, for Injector 5, it was necessary to install the transducers behind taps approximately 1.06 in. long and 0.187 in. in diameter. Consequently, it should be noted that the amplitude response of those latter measurements is suspect to the extent that the measurements include the resonance contribution of the tap. Shock-tube experiments with similar geometries have indicated appreciable resonance (cavity, tap, transducer) with peaks in the range of 6 times in the neighborhood of the 2500 Hz natural frequency.

The results obtained from tests with these two injectors are summarized in the tables of Figs. 14 and 15. The figures include a portion of typical pressure records as well as a summary of the geometrical and time relationships of the measurements. Starting from an arbitrary geometrical position of any one measurement, it is seen (as indicated in the last column of the table) that, within the accuracy limits of the data, the phase relationship and geometrical position for any one axial station are essentially identical. However, a comparison of data at the two different stations shows a definite lag in the arrival of the disturbance at the injector plane. This lag varies for the two different propellant-injector configurations, as do the characteristic periods of the disturbance and, to a lesser extent, the pressure ratio of the disturbance. The average characteristics of the disturbance, as indicated in the figures, clearly show that (1) the local pressure ratio across the disturbance is in the range of 4 to 10 times, (2) the velocity of the intersection of the disturbance with the boundary is almost 7000 ft/s, (3) the front is steep, with the disturbance comprising approximately 20% of the period, and (4) the peak amplitude of the disturbance at any point varies only slightly with time. As indicated in the discussion of results, it is extremely difficult to rationalize these observations in terms of a rotating, transverse acoustic wave.

It should be noted that neither the true maximum amplitude nor the spatial characteristics of this disturbance are indicated in these recorded analogues. In a separate experiment conducted by S. Rogero (Ref. 8), the time history of the disturbance at the boundary was determined with a relatively high-response ($f_r \stackrel{a}{=} 150$ kHz) Kistler transducer with the output driving an oscilloscope and the trace recorded on Polaroid film (i.e., a random disturbance recorded directly from the oscilloscope). A typical record thus obtained and reported in Ref. 8 is shown in Fig. 16 where it is compared to similar recordings (although not necessarily the same pulse) from the usual Photocon transducer as well as a transducer manufactured by Dynisco. These records are compared to those obtained with the standard FM tape recording and playback system and, finally, with an analogue of an electronically generated square wave as attenuated by that same FM tape system. These data show that the rise time of the front is not more than a few microseconds (which at the velocity of the disturbance boundary intersection is also nearly the transit time of a line across the transducer) and that the rounded characteristics of the records

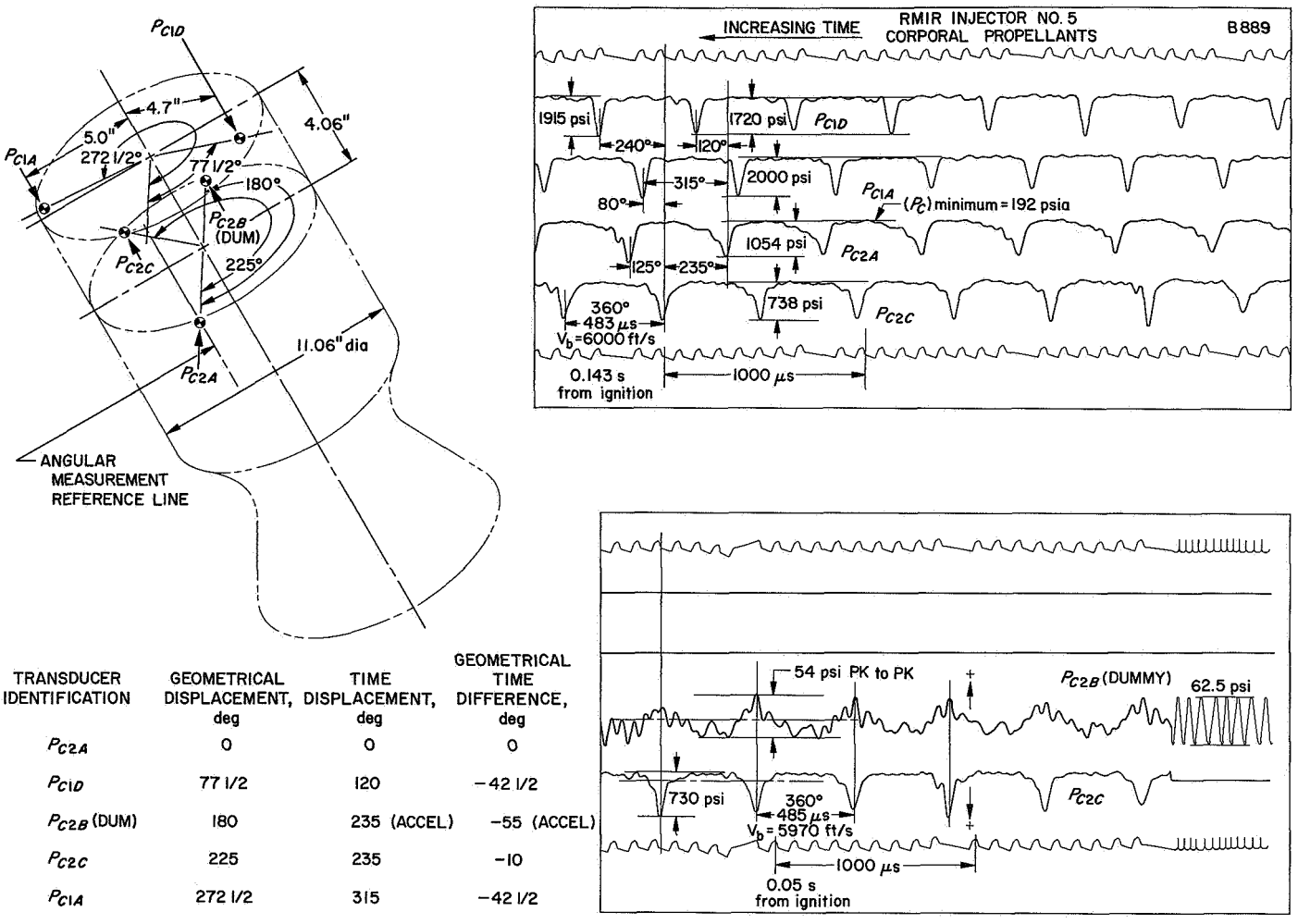

TRANSDUCER IDENTIFICATION	GEOMETRICAL DISPLACEMENT, deg	TIME DISPLACEMENT, deg	GEOMETRICAL TIME DIFFERENCE, deg
P_{C2A}	0	0	0
P_{C1D}	77 1/2	120	−42 1/2
P_{C2B} (DUM)	180	235 (ACCEL)	−55 (ACCEL)
P_{C2C}	225	235	−10
P_{C1A}	272 1/2	315	−42 1/2

Fig. 14. Phase measurements for resonant combustion for RMIR Injector 5 with *Corporal* propellants

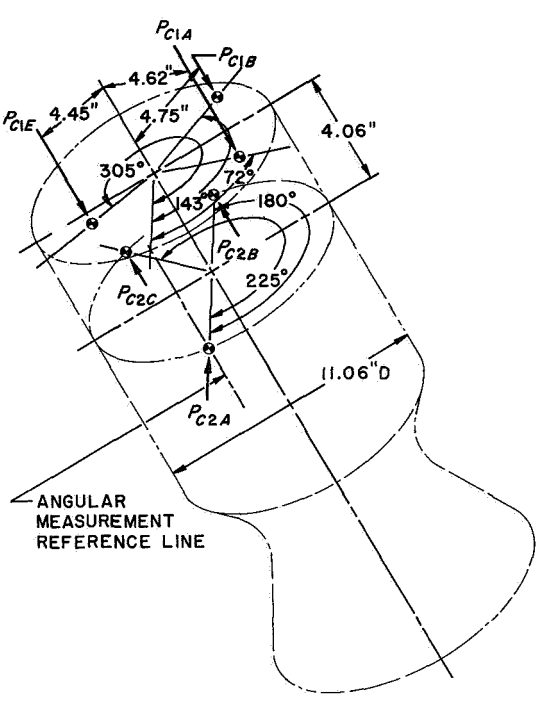

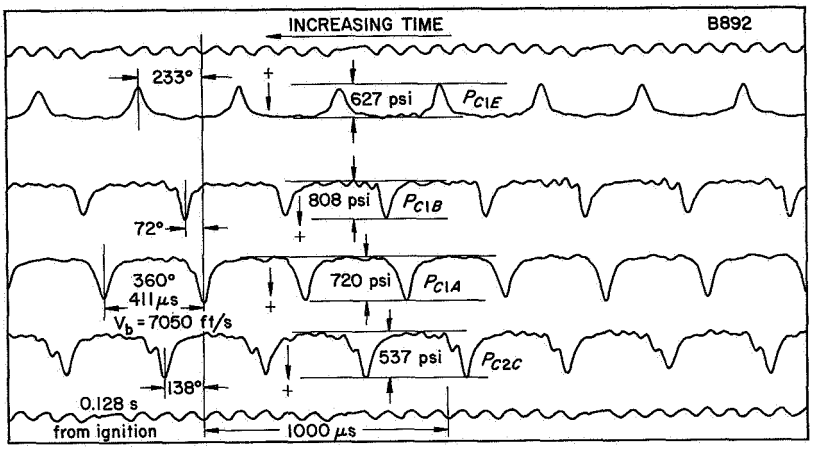

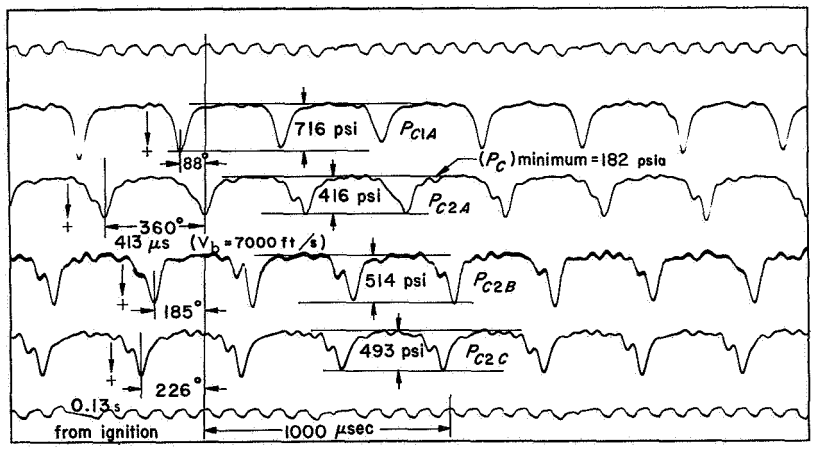

TRANSDUCER IDENTIFICATION	GEOMETRICAL DISPLACEMENT, deg	TIME DISPLACEMENT, deg	GEOMETRICAL TIME DIFFERENCE, deg
P_{C2A}	0	0	0
P_{C1A}	72	88	-16
P_{C1B}	143	160	-17
P_{C2B}	180	185	-5
P_{C2C}	225	226	-1
P_{C1E}	305	321	-16

Fig. 15. Phase measurements for resonant combustion for RMIR Injector 7 with N_2O_4 and N_2H_4 as propellants

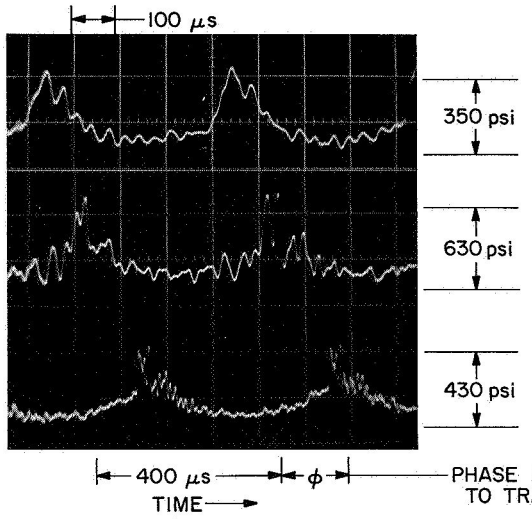

(a) PHOTOGRAPH OF OUTPUT OF DYNISCO (TOP), PHOTOCON (CENTER), KISTLER (BOTTOM) DIRECT FROM TRANSDUCER-PRIOR TO RECORDING ON TAPE

"NOISE" MAY BE PARTIALLY DUE TO TRANSDUCER RINGING

PHASE DIFFERENCES ARE TYPICALLY PROPORTIONAL TO TRANSDUCER DISPLACEMENT

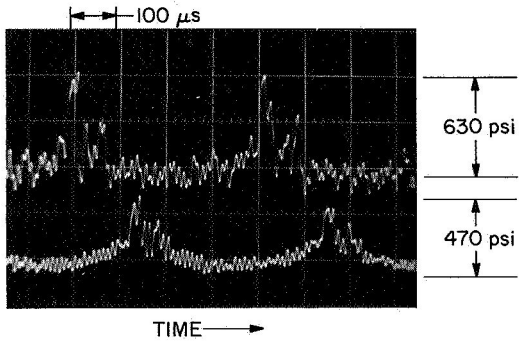

(b) PHOTOGRAPH OF OUTPUT OF PHOTOCON (TOP), KISTLER (BOTTOM), AFTER DIRECT RECORDING AND PLAYBACK ON TAPE AT 60 ips

100 kHz NOISE INTRODUCED BY TAPE

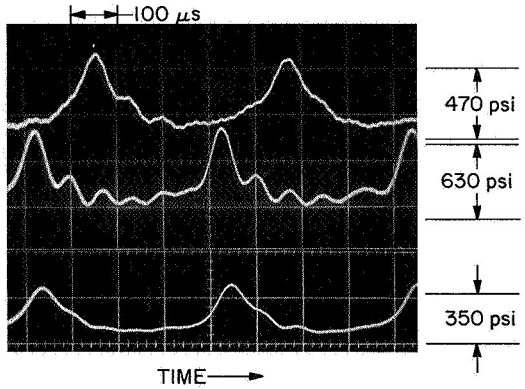

(c) PHOTOGRAPH OF KISTLER (TOP), PHOTOCON (CENTER), DYNISCO (BOTTOM) AT 3 3/4 ips PLAYBACK AFTER FM RECORDING AT 60 ips

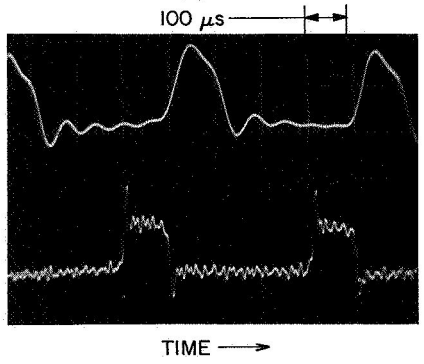

(d) INPUT TO RECORDER WAS SQUARE PULSE OF 100 μs DURATION

TOP TRACE: FM

LOWER TRACE: DIRECT (AM)

Fig. 16. Spatial characteristics of resonant wave

shown in Figs. 14 and 15 actually represent the response capability of the recording system, i.e., limited to approximately 10 kHz. The amplitude determined by the Kistler transducer is somewhat lower than that indicated by the Photocon transducer, particularly after FM recording and slow playback (Part c, Fig. 16). Obviously, this is in the direction of attenuation caused by response limitations of the tape system but really serves only to indicate the problems associated in obtaining quantitative amplitude information.

J. Heat Transfer During Resonant Combustion

The steady state heat-transfer characteristics of the injector-propellant combinations evaluated as part of the RMIR Project are presented in Ref. 4. However, it should be noted that a substantial increase in local heat transfer accompanied the transition to the resonant mode. This was particularly true near the injector face and/or along the chamber near the injector end. As might be expected, this was the same area that experienced the extremely severe erosion shown in Fig. 3. It should also be noted (Ref. 4) that a direct quantitative comparison of chamber heat-transfer characteristics for two different configurations, the two combustion modes of interest here, is quite difficult. Complications arise because of (1) the transient nature of the heat-transfer measurement, which produces a more or less continuously changing wall temperature, (2) the extremely large gradients that exist in the chamber during steady state combustion that, in turn, make it difficult to choose a representative average value for any one station, (3) the possibility that energy released by direct oxidation and/or recombination reactions at the wall during the resonant mode contribute to the apparent heat-transfer rate, and (4) the time interval for which measurements can be obtained during resonant combustion is marginal with respect to achieving stability in the computer calculation of heat-transfer rates. Nevertheless, even with the limited amount of available information, it is possible to indicate the trends shown in Figs. 11 and 12 of Ref. 4, reproduced here as Figs. 17 and 18, together with the following textual material from that reference: "The onset of resonant combustion is identified by an abrupt change in the rate of temperature change with time throughout the chamber. Fig. 17 shows the temperature-time history at a given chamber location for several significantly different resonant environments and compares them with a typical nonresonant transient. In each case, the heat flux associated with several particular times during the transient is indicated. It should be noted that, with RMIR Injector 5, the addition of a subcritical-length baffle reduced the amplitude of the disturbance from approximately 1500 psi to approximately 200 psi, but reduced the heat flux by only 25%. Further, the extension of the length of the baffle by an additional inch reduced the pressure disturbances to a negligible value and produced a large decrease in heat flux. The overall effect is to produce a decrease of almost an order of magnitude in heat flux as the transition from resonant to nonresonant combustion takes place.

"Figure 18 is an attempt to illustrate the variations in the axial distributions that occur for those same variations in operating conditions. It is clear that the scatter in the data precludes any truly definitive conclusions. However, the same general relationships shown in Fig. 17 prevail at any given axial station and, additionally, there is a progressive change in the characteristics of the axial distribution as the severity of the disturbance increases. In particular, the heat flux tends toward a maximum at the nozzle inlet with stable combustion, while the maximum occurs near the injector end of the chamber during resonant combustion. Moreover, the magnitude of the heat flux at the nozzle inlet tends toward a common value, indicating the establishment of similar boundary conditions, presumably because similar, near-equilibrium velocities are attained in both combustion modes. It should further be noted that local variations in the mass distribution, either in the chamber or on the chamber walls, tend to be overwhelmed by these high-amplitude disturbances and, therefore, have little or no effect upon heat-transfer data obtained during unstable combustion."

"For reference purposes only, these figures also include comparable heat-transfer characteristics obtained with a somewhat different injection scheme (RMIR 7), using the propellant combination N_2O_4 and N_2H_4. The heat flux for this system during resonant combustion is somewhat lower than that for the RMIR Injector 5, *Corporal* propellant system."

The data are much too crude to provide information on the transient heat-transfer characteristics; however, if it is assumed that (1) the average values (for multiple oscillations) are linear combinations of the heat transfer during the high-pressure region of the disturbance (assumed to have constant properties for some 20% of the period of the wave) and the low-pressure region, and (2) the heat-transfer rate during the low-pressure portion of the wave can be characterized by the steady state heat-transfer rate, then it can be shown (calculations below and Fig. 19) that the heat-transfer rate during the high-pressure part of the period (for typical values) is essentially five times the average value and the ratio of heat transfer between high-pressure and low-pressure

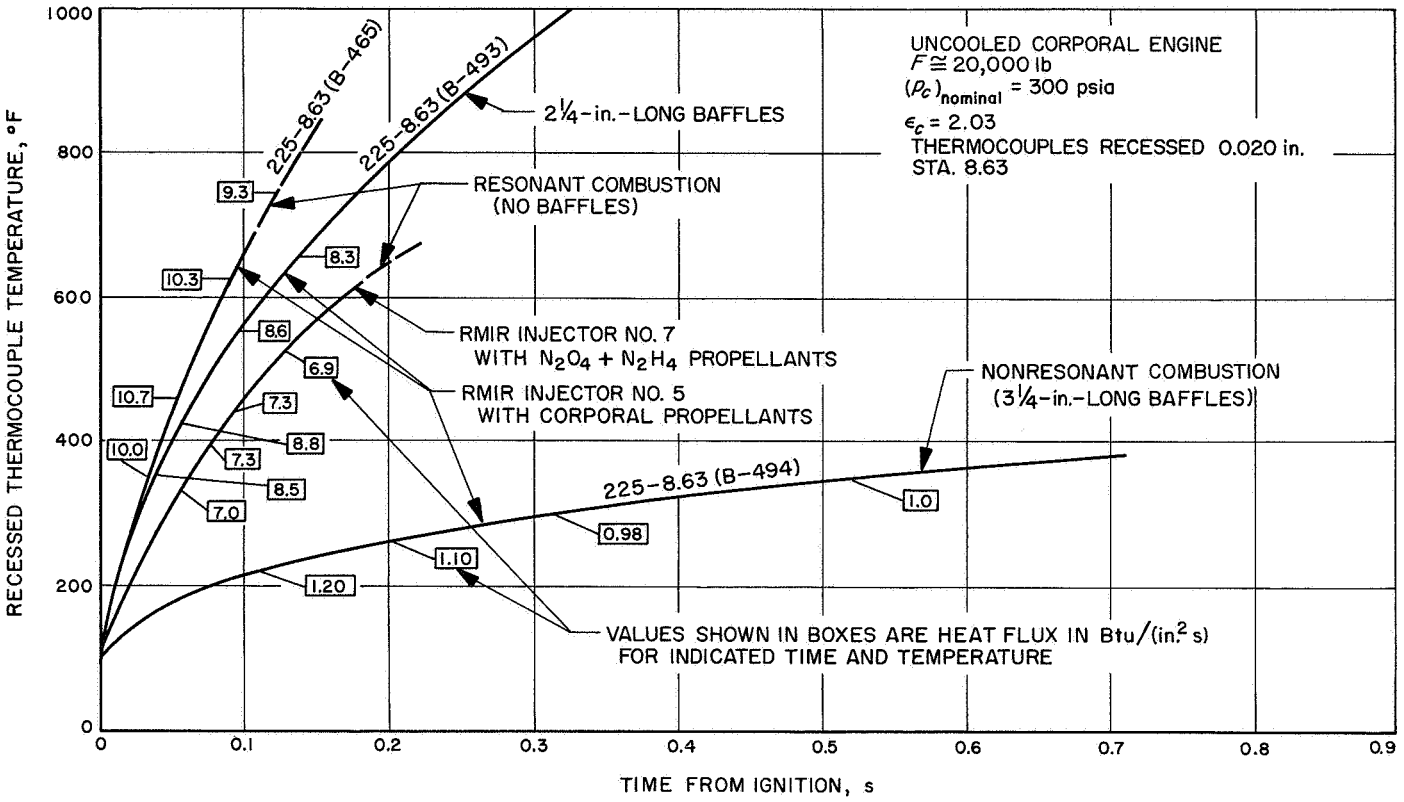

Fig. 17. Variations in heat transfer due to resonant combustion for a particular chamber location

portions of the period would have to be approximately 146. The following shows this reasoning:

Assume

$$0.2q_1 + 0.8q_{min} = q_{av} \qquad (1)$$

$$q_{min} = q_{ss} \qquad (2)$$

From experiment

$$q_{ss} \overset{a}{=} 0.5 \text{ Btu/in.}^2 \text{ s}$$

$$q_{av} \overset{a}{=} 16 \text{ Btu/in.}^2 \text{ s}$$

and

$$\frac{q_{av}}{q_{ss}} = 32 \text{ or } q_{ss} = \frac{q_{av}}{32}$$

Then, from Eq. (1)

$$0.2q_1 + 0.8\,\frac{q_{av}}{32} = q_{av}$$

$$q_1 = \frac{39}{8}\,q_{av}$$

Since

$$q_2 = \frac{q_{av}}{32}$$

$$\frac{q_1}{q_2} = 146$$

It should be noted that, under these conditions, the wall temperature is changing at the rate of some 20,000°/s. Therefore, it is not surprising that an engine can literally cut itself loose from the injector flange in a few hundred milliseconds when an inadvertent transition to the resonant mode takes place. As will be seen later, the fact that the heat-transfer rates approach each other at the nozzle inlet is consistent with the concept of a detonation-like disturbance traveling in a circumferential path near the injector, producing a highly disassociative composition that decays toward equilibrium composition and state conditions as the reaction products flow toward the nozzle inlet.

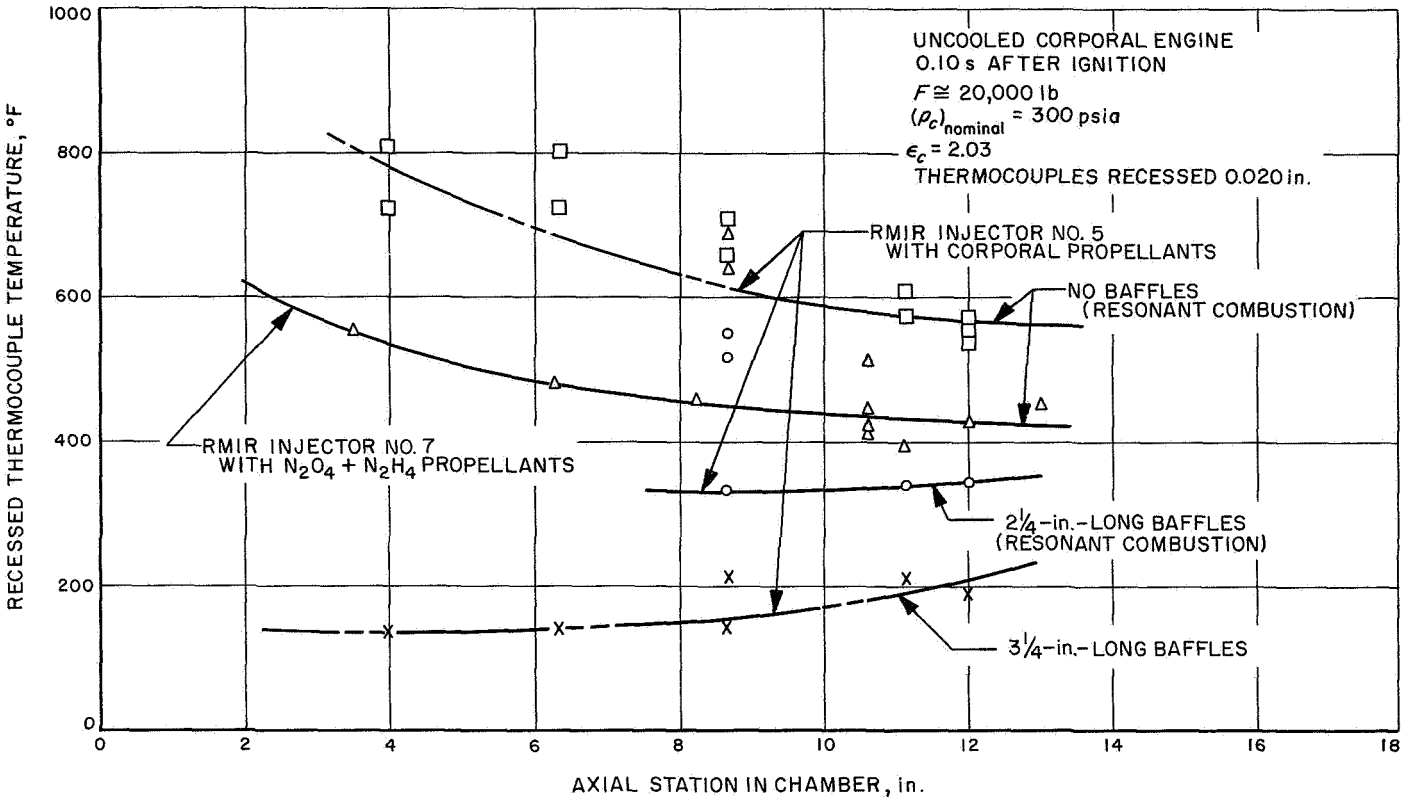

Fig. 18. Variations in transient temperature distributions due to resonant combustion

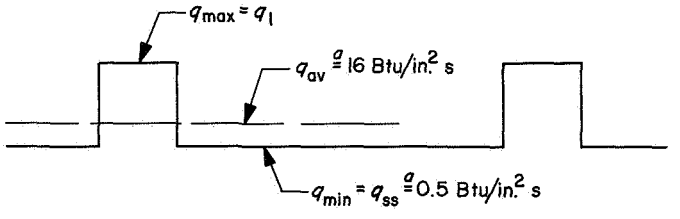

Fig. 19. Idealized wave form

V. Discussion of Results and Concluding Remarks

Resonant combustion in rocket engines has generally been characterized in terms of the acoustic properties of the chamber-nozzle geometry. This is, for example, the approach taken by Professor Crocco and coworkers at Princeton (Ref. 12), Preim at Lewis (Ref. 13), Levine, et al., at Rocketdyne (Ref. 14), and is the basis for Barr'ere's discussions in Ref. 13. Further, a number of experiments, including those of Berman and Cheney (Ref. 15), Zucrow, et al. (Ref. 16), and others, have demonstrated the existence of such waves. Therefore, the existence of this family of disturbances is not denied, nor is it implied that the transition from the initial disturbance to the fully developed resonant wave may not be of this type. However, it is difficult to reconcile the data presented herein with the boundary conditions imposed on acoustic disturbances (Ref. 17). It is therefore suggested that these disturbances are much better represented by the detonation-like disturbance[3] discussed by Nicholls, et al., and described in a more phenomenological sense by Krieg (Ref. 18). The measurements reported herein seem to support the data of Krieg if certain allowances are made for the individual evaluations of the spatial characteristics of the wave. The differences in pressure ratio across the front must, in part, be attributed to instrumentation problems (e.g., differences in response limitations for individual systems); however, it is more likely that these problems stem from the differences in injection schemes, propellant characteristics, and, according to Krieg, "the energy available for consumption in the front." The injection schemes utilized in the experiments

[3] *Detonation-like disturbance* is used in the sense defined by Jost (Ref. 19, p. 161): "this compression of the fresh gas (required to accelerate the burnt gases to a high velocity) produces a shock wave that progresses with a velocity greater than sound, and the burning zone is coupled with the front of this wave. This process is called *detonation*."

reported herein were intended to produce nearly uniform axial mass flux and mixture ratio distributions and, coincidently, yielded relatively high average-mass fluxes (in the range of 1 lb/s in.^{2}) Krieg's injectors concentrated the relatively unmixed propellants (showerhead injector) near the outer boundary and, presumably, produced relatively low-axial mass fluxes (in the range of 0.10 lb/s in.^{2}).

Figure 16 shows that the rise time produced by the passage of the front can be in the range of 4–6 μs. Because this is also the approximate transit time of the wave across the face of the transducer, this time cannot, even in this case, be interpreted as a true measure of the thickness of the front. It is therefore suggested that similar considerations of the response capabilities of Krieg's instrumentation system might reduce his estimate for the thickness of the front from 1.2 in. to a much smaller value.

The simultaneous pressure measurements summarized in Figs. 14 and 15 also verify Krieg's conclusion that the disturbance is "a continuous single-front instability... propagating circumferentially around the chamber." Although Krieg's data indicated the existence of multiple fronts, this was not apparent in JPL's smaller chamber.

In general, these concepts are contained in the theoretical description of the rotating detonation wave engine postulated by Nicholls, et al.[4] (Ref. 20). The major difference lies in the geometry of Nicholls' engine which is essentially a cylindrical annulus with an end aperture rather than the full cylinder with one end more or less open which is usually used as a rocket engine. In the case chosen by Nicholls, the flow can be approximated by a one-dimensional linear tube with a rectangular cross section. This simplifies the analysis so that the working equations given in Ref. 20 can be derived. However, it should be noted that Nicholls demonstrated experimentally that a detonation wave can turn in response to pressure gradients imposed by a wall and a relief (Ref. 20, Fig. 37) as is required for a rotating wave.

Therefore, it seems appropriate to describe the disturbance observed as a detonation-like wave driven continuously by the energy available from the injected propellants, but constrained by the geometrical boundaries of the chamber and the complicated flow field resulting from the disturbance and the mean axial flow down the chamber. The local properties of the disturbance are undoubtedly related to the local environments so that both local velocity as well as amplitude of the disturbance will vary with position in the chamber. Further, it would appear that the reaction-supported part of the disturbance is concentrated in the volume near the injector (since periods are consistent with injection distances of an inch or less) so that the amplitude and mach number of the wave would be expected to decrease with axial distance. Also, the predominantly circumferential motion of the pressure wave, always in one direction, implies a corresponding gas velocity, hence a vortex flow with its associated pressure and velocity distribution as well as its complex boundary flow. Therefore, the disturbance does not depend upon acoustic coupling for its sustenance and could be associated with one of the "other mechanisms" as imagined by Crocco and Cheng (pp. 17–18, Ref. 11).

As noted in previous sections, the consequences of a sustained disturbance of this type are certainly consistent with experience. The extremely severe heat-transfer rates and erosion rates that are preferentially located near the injector face are consistent with the high-pressure ratios (as high as 10) of these disturbances. Also, when such pressures exist, the probability for dissociation in the wave with recombination at the wall is high, and the protective boundary layer, essential for wall compatibility, is essentially nonexistent as long as these high-velocity shock-like disturbances continue to scrub the wall.

Therefore, for real systems, where propellant loading densities are relatively large, it may be possible to drive an extremely destructive disturbance (insofar as a chamber boundary is concerned) without ever involving an acoustic coupling. The bounds of the environment conducive to such disturbances must be defined, the mechanism of transition from the unstable combustion mode to the oscillating (or resonant) mode must be elucidated, and means for control and elimination of such disturbances must be devised.

[4]These theoretical concepts are supported by some early experiments by Cosens (and others) (see Machine Design, May 25, 1961, p. 23) and the recent experiments that are serving to verify Nicholls' original postulates.

References

1. Rupe, J. H., *An Experimental Correlation of the Nonreactive Properties of Injection Schemes and Combustion Effects in a Liquid-Propellant Rocket Engine: Part I. The Application of Nonreactive-Spray Properties to Rocket-Motor Injector Design.* Technical Report 32-255, Jet Propulsion Laboratory, Pasadena, Calif., July 15, 1965.

2. Clayton, R. M., Rupe, J. H., and Gerbracht, F. G., *An Experimental Correlation of the Nonreactive Properties of Injection Schemes and Combustion Effects in a Liquid-Propellant Rocket Engine: Part II. On Instrumentation, Experimental Apparatus, and Experimental Techniques,* Technical Report 32-255, Jet Propulsion Laboratory, Pasadena, Calif., May 15, 1967.

3. Rupe, J. H., *An Experimental Correlation of the Nonreactive Properties of Injection Schemes and Combustion Effects in a Liquid-Propellant Rocket Engine: Part III. On the Relation Between Gross Performance Level and Injection Scheme,* Technical Report 32-255, Jet Propulsion Laboratory, Pasadena, Calif. (to be published).

4. Jaivin, G. I., Rupe, J. H., and Clayton, R. M., *An Experimental Correlation of the Nonreactive Properties of Injection Schemes and Combustion Effects in a Liquid-Propellant Rocket Engine: Part IV. Relating Heat Transfer to the Chamber Wall and the Injection Pattern,* Technical Report No. 32-255, Jet Propulsion Laboratory, Pasadena, Calif. (to be published).

5. Clayton, R. M., and Rupe, J. H., *An Experimental Correlation of the Nonreactive Properties of Injection Schemes and Combustion Effects in a Liquid-Propellant Rocket Engine: Part VI. The Relation Between the Starting Transient and Injection Hydraulics,* Technical Report 32-255, Jet Propulsion Laboratory, Pasadena, Calif., Oct. 29, 1965.

6. Rupe, J. H., *An Experimental Correlation of the Nonreactive Properties of Injection Schemes and Combustion Effects in a Liquid-Propellant Rocket Engine: Part VII. The Performance Characteristics of Injection Schemes Utilizing High-Flow Rate Elements,* Technical Report 32-255, Jet Propulsion Laboratory, Pasadena, Calif. (to be published).

7. Nerheim, N. M., *An Experimental Correlation of the Nonreactive Properties of Injection Schemes and Combustion Effects in a Liquid-Propellant Rocket Engine: Part VIII. On the Experimental Performance of the Pentaborane-Hydrazine Propellant Combination,* Technical Report 32-255, Jet Propulsion Laboratory, Pasadena, Calif., April 30, 1962 (Confidential).

8. Rogero, S., *Measurement of the High-Frequency Pressure Phenomena Associated with Rocket Motors,* Technical Report 32-624, Jet Propulsion Laboratory, Pasadena, Calif., May 11, 1964.

9. Research Summary 36-9, Vol. I, pp. 82–84, Jet Propulsion Laboratory, Pasadena, Calif., July 1, 1961.

10. Rowley, R. W., *An Experimental Investigation of Uncooled Thrust-Chamber Materials for Use in Storable Liquid-Propellant Rocket Engines,* page 8, Technical Report 32-561, Jet Propulsion Laboratory, Pasadena, Calif., Feb. 15, 1964.

References (contd)

11. Crocco, L., and Cheng, Sin-I, *Theory of Combustion Instability in Liquid-Propellant Rocket Motors,* Butterworths Scientific Publications (1956).

12. Crocco, L., "Theoretical Studies on Liquid-Propellant Rocket Instability," *Tenth Symposium (International) on Combustion,* The Combustion Institute, pp. 1101–1128, 1965.

13. Barr'ere, M., and Jaumotte, A., *Rocket Propulsion,* Elsevier Publishing Company, New York, 1960.

14. Levine, R. S., "Experimental Status of High-Frequency Liquid-Rocket Combustion Instability," *Tenth Symposium (International) on Combustion, The Combustion Institute,* pp. 1083–1099, 1965.

15. Berman, K., and Cheney, S. H., Jr., "Rocket Motor Instability Studies," in *Jet Propulsion,* Vol. 25, No. 10, Oct. 1955.

16. Zucrow, M. J., Osborne, J. R., and Bonnell, J. M., *Summary of Experimental Investigations of Combustion Pressure Oscillations in Gaseous Propellant Rocket Motors,* Final Report F-63-2 (Contract AF49 (638)-756), Jet Propulsion Center, Purdue University.

17. Beranek, L. L., Acoustics, page 22, McGraw-Hill Book Co., Inc., New York, (1954).

18. Krieg, H. C., Jr., "Tangential Mode of Combustion Instability," *Detonation and Two-Phase Flow,* (p. 339), Academic Press (New York-London), 1962.

19. Jost, W., *Explosion and Combustion Processes in Gases,* McGraw-Hill Book Co., Ltd. (First Edition).

20. Nicholls, J. A., and Cullen, R. B., et al., *The Feasibility of a Rotating Detonation Wave Rocket Motor,* Technical Documentary Report RPL-TDR-64-113, Air Force Flight Test Center (6593d Test Group) USAF, Edwards AFB, Calif., April 1964.

21. Male, T., and Kerslake, W. R., *Methods of Prevention of Screaming in Rocket Engines,* NACA Report RME 54F 28A, 1954.